A Comprehensive Review on Polymer-Dispersed Liquid Crystals: Mechanisms, Materials, and Applications

Shikha Agarwal, Swastik Srivastava, Suraj Joshi, Shivangi Tripathi, Bhupendra Pratap Singh, Kamal Kumar Pandey,* and Rajiv Manohar*

Cite This: ACS Mater. Au 2025, 5, 88−114

Read Online

ACCESS | Metrics & More | Article Recommendations | Supporting Information

ABSTRACT: Polymer-dispersed liquid crystals (PDLCs) stand at the intersection of polymer science and liquid crystal technology, offering a unique blend of optical versatility and mechanical durability. These composite materials are composed of droplets of liquid crystals interspersed in a matrix of polymeric materials, harnessing the optical properties of liquid crystals while benefiting from the structural integrity of polymers. The responsiveness of LCs combined with the mechanical rigidity of polymers make polymer/LC composites—where the polymer network or matrix is used to stabilize and modify the LC phase—extremely important for scientists developing novel adaptive optical devices. PDLCs have garnered significant attention due to their ability to modulate light transmission properties, making them ideal candidates for applications ranging from smart windows and displays to light shutters and privacy filters. The incorporation of different ferroelectric, thermoelectric, magnetic, and ferromagnetic nanoparticles, quantum dots, nanorods, and a variety of dyes in the PDLC matrix has gained momentum over a span of few decades, as it lowers the otherwise-required high operating voltage and reduces the electro-optical response time of these devices. Due to better contrast in the transmittance of these materials in the field-off and on states, they find extensively wide application in a variety of photonic applications, viz., optical shutters and smart windows, photorefractives, modern displays, microlens arrays encompassing polymer-gravel lenses, and many other. Since the functional parameters of these devices embrace the thermophysical attributes of PDLC networks, it therefore becomes necessary to perform a detailed analysis of the properties of PDLCs and their ameliorations upon the addition of different dopants. This Review aims to review the recent advances in PDLCs and their enrichment in terms of their performance parameters upon the addition of a variety of dopants, as well as the improvement of different photonic applications owing to superior parametric implementation of these networks.

KEYWORDS: polymer-dispersed liquid crystals (PDLCs), phase separation techniques, polymer-gravel lenses, PDLC based sensors, smart windows, normal-mode PDLCs (NPDLCs), polymer-stabilized liquid crystals (PSLCs), nematic liquid crystals
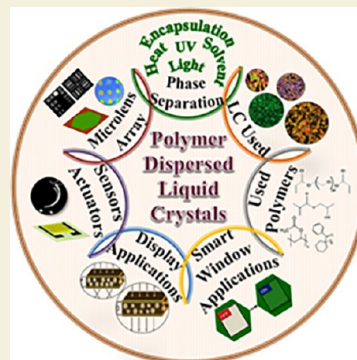
1. INTRODUCTION

Liquid crystalline (LC) materials have been a topic of extensive research for a variety of scientific and technological applications for more than a century due to their remarkable optical and dielectric anisotropy. External stimuli like electric and magnetic fields are capable of causing molecular reorientations in the LC matrix by virtue of electric torque exerted on the induced dipoles in LC molecules.[1] The traveling speed of a light wave incident on uniformly aligned LC molecules is altered on account of the optical anisotropy of the material, the angle of incidence of the light wave, and its state of polarization. These splendid properties make LCs a promising choice for different industrial and nonindustrial applications like spatial light modulators, flexible and dual-view displays,[2−4] 2D/3D autostereoscopic displays and HD screens,[5−8] adaptive lens technologies and smart windows,[9−13] augmented reality,[14,15] different terahertz (THz) devices, etc.[10,16] However, certain limitations inherent to the inclusion of these materials in practical devices include the requirement

of alignment layers because of the anisotropic behavior being dependent on the alignment and anchoring conditions of LC molecules.[17−19] Also, the requirement of polarizers with these materials limits their applicability, as the polarizers absorb a large portion of transmitted light. This reduction of the transmitted light intensity affects the electro-optical properties of LCs adversely. Several guest entities like nanoparticles, quantum dots, dyes, nanorods, chiral compounds, and many others possess the capability to enhance this anisotropic behavior and tune the properties of liquid crystals through interaction.[12,20−25] The purpose of exploring the guest−host interaction with LC molecules is to control their optical
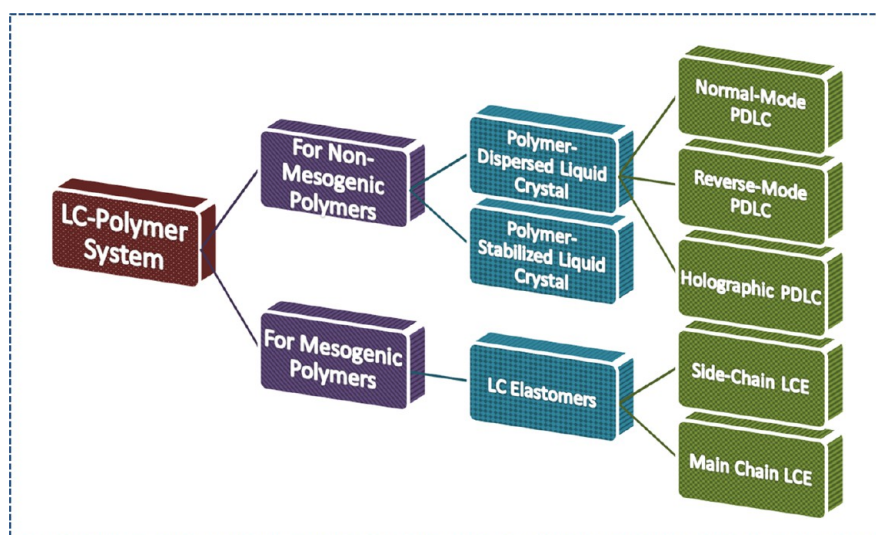
Figure 1. Classification chart of LC−polymer composite systems.
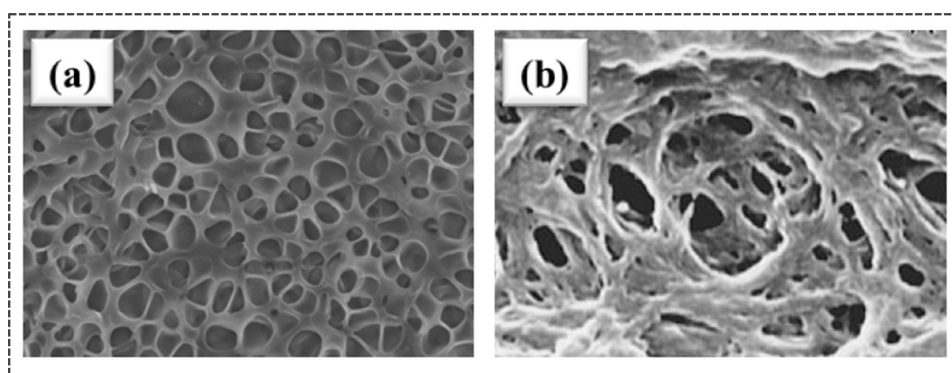
Figure 2. SEM images exhibiting the morphology of (a) a polymer-dispersed liquid crystal and (b) a polymer-stabilized liquid crystal. (a) Reproduced from ref 33. Available under a CC-BY license. Copyright 2019 H-Q Zhang and H. Yang et al. (b) Adapted with permission from ref 34. Copyright 1996 American Chemical Society.

properties using an external electric or magnetic field. Few researchers also explored this field by confining or dispersing liquid crystalline droplets in anisotropic solids or isotropic liquids.[26,27]

In this regard, the idea of using polymeric films with LC droplets embedded into them was proposed and studied further by different researchers.[28−30] Polymers consist of long chains of identical units, often known as monomers, flexibly joined to each other. The interactions of polymers and liquid crystals depend on several parameters, such as the amount in which they are combined, the technique of phase separation, the extent of polymerization, and others.[31]

As shown in Figure 1, liquid crystal−polymer composite systems can be broadly categorized in two ways depending on whether the polymeric chain itself shows liquid crystallinity. For nonmesogenic polymers, in accordance with the morphology of the derived system, LC−polymer composites (LCPCs) belong to two classifications: polymer-stabilized liquid crystals (PSLCs) and polymer-dispersed liquid crystals (PDLCs), with the former having very small content of polymers (generally lower than 10%) and the latter consisting of polymers and liquid crystals in almost comparable concentrations.[32] This difference in the amount of polymers in these two subgroups of LCPCs changes the morphology of

the prepared composites and has been illustrated with the help of SEM images, as shown in Figure 2a and b.

A continuous matrix of properly phase-separated polymer tends to incorporate liquid crystalline droplets into itself in the case of PDLCs, whereas for preparing PSLCs the LC is dispersed with a photoreactive monomer whose molecules align themselves along the director of the LC. The two situations can also be clearly seen in Figure 2. The large pores in the microscopic image shown in Figure 2a represent the regions of LC droplets formed in the continuous polymer matrix (seen in the image as mesh surrounding the large domains of LC droplets) after phase separation during polymerization.[33] Smooth polymer strands in the liquid crystalline matrix can be observed in case of PSLC systems, as shown in Figure 2b.[34] From the point of view of practical applications, the liquid crystal−polymer composites (LCPCs) have proven their utility in different sectors like optical fiber telecommunications, optical shutters, spatial light modulators, switchable windows, etc.[35−43]

Apart from these two classifications, a whole new category of LC−polymer systems came to light with the incorporation of a mesogenic group into the polymer structure, i.e., when the polymer itself exhibits mesogenic properties. These systems are termed as LC elastomers and can be further classified into two groups depending on the position of the mesogenic group: the

mesogenic moieties can be either attached as a side chain to the monomer (side-chain elastomers) or directly linked within the polymer (main-chain elastomer). These systems find great utility in soft actuators, microelectric-mechanical systems, artificial muscles, etc.[44−46] Different research groups have beautifully reviewed the properties and scope of applicability of these materials.[47−49] Therefore, to maintain the comprehensive nature of this Review, further discussions will be limited to PDLCs only.

Polymer-dispersed liquid crystals (PDLCs) represent a cutting-edge class of materials that are at the forefront of modern optics and materials science. These composite materials combine the unique optical properties of liquid crystals with the mechanical resilience of polymers, offering versatile solutions for light modulation, display technologies, and beyond.[50−53] PDLCs have garnered significant interest and applications across various industries due to their ability to dynamically control light transmission and scattering properties, making them integral components in smart windows, display devices, privacy filters, and adaptive optics.[54−59] PDLCs are engineered materials with LC droplets having dimensions of micrometers dispersed within a solid polymer matrix. In PDLCs, the LC droplets are suspended in a polymer matrix, forming a heterogeneous structure where the optical behavior can be controlled by external stimuli such as electric fields, temperature changes, or mechanical stress.[60,61] The morphology and distribution of liquid crystal droplets within the polymer matrix play a crucial role in determining the optical and mechanical properties of PDLCs.[62] The formation of PDLCs typically involves dispersing liquid crystal molecules, which are often rod-shaped and anisotropic, into a polymer solution or melt. Upon phase separation, the liquid crystal molecules nucleate and grow within the polymer matrix, forming droplets with diameters ranging from nanometers to micrometers.[63] The size, shape, and spatial distribution of these droplets significantly impact the optical response of the PDLCs. Small, uniformly dispersed droplets tend to enhance the optical clarity in the transparent state, while larger or more clustered droplets may induce light scattering and opacity. The optical behavior of PDLCs arises from the unique interaction between liquid crystal droplets and external stimuli. In their transparent state, PDLCs align their liquid crystal domains to minimize light scattering, allowing light to pass through with minimal distortion. This transparency can be rapidly altered by applying an electric field,[64] which reorients the liquid crystal molecules within the droplets, causing them to scatter light and turn the PDLC opaque. Such electro-optical switching mechanisms enable PDLCs to function as dynamic light control devices, finding applications in glare reduction systems, privacy windows, and adaptive optics. Beyond static light modulation, PDLCs exhibit tunable optical properties that can be tailored to specific applications. By adjusting parameters such as liquid crystal composition, polymer matrix type, and droplet size distribution, researchers can optimize PDLCs for enhanced contrast, faster response times, and broader wavelength sensitivity. Advances in material synthesis and fabrication techniques have led to the development of PDLC variants with improved optical clarity, lower operating voltages, and extended durability, expanding their utility in consumer electronics, automotive glass, and architectural coatings.

PDLCs represent a transformative class of materials with unparalleled capabilities in optical modulation and light control. By harnessing the synergistic properties of liquid crystals and polymers, PDLCs offer scalable solutions for diverse applications, ranging from smart windows and displays to advanced optical sensors and light management systems. Research on PDLCs is crucial for advancing technology in a variety of industries. Characterizing the optical and mechanical properties of PDLCs is essential for optimizing their performance and reliability in practical applications. Techniques such as optical microscopy, spectroscopy, and ellipsometry provide insights into droplet morphology, refractive index matching between phases, and electro-optical response dynamics. Mechanical testing, including tensile strength measurements and durability assessments under varying environmental conditions, ensures that PDLCs meet performance standards for long-term operation in harsh or dynamic environments. Important relevant research on polymer-dispersed liquid crystals is in smart windows, photorefractives, soft actuators, ultrasound imaging, bioimaging, responsive sensors, dynamic optical regulation windows, etc.[65−70] Until now, PDLC films have been established to offer superior mechanical and electro-optical qualities.[71−73] This research can lead to advancements in fields such as healthcare, telecommunications, and energy efficiency, and it is essential for creating innovative and efficient products that can positively impact the overall health and well-being of occupants. Though the PDLC systems have certain shortcomings, such as the requirement of high driving voltage, longer response time, optimization of phase separation technique, etc., that limit their commercial applications, several attempts in this field are continuously made by different research groups to overcome these drawbacks and increase the commercial utility of these systems. The vast literature available on the ongoing research on PDLCs necessitates some comprehensive reviews to provide a complete and systematic summarized comparative analysis dedicated to this field.

In this Review, we delve into the fundamental principles governing the behavior of PDLCs, from the formation and morphology of liquid crystal droplets within the polymer matrix to the mechanisms underlying their optical response. Understanding the chemistry and physics of these macromolecules is a prerequisite for the development and application of new materials in the current scenario. With this aim, we explore recent advancements in PDLC technology, including novel fabrication techniques and emerging applications across different industries. Furthermore, we discuss challenges in PDLC research, such as achieving uniform droplet distribution and improving response times, and we propose future directions for optimizing their performance and expanding their functional capabilities. By synthesizing current research and technological developments, this Review aims to provide a comprehensive overview of PDLCs, highlighting their potential as dynamic materials for next-generation optical devices and beyond.

2. THEORY OF LIQUID CRYSTAL−POLYMER COMPOSITES

The fundamental principle underlying PDLCs lies in the control of the liquid crystal orientation within a solid polymer matrix. Liquid crystals exhibit distinct optical characteristics based on their molecular alignment, which can be influenced by external electric fields, temperature changes, and mechanical stress. In PDLCs, liquid crystal droplets are dispersed at a microscopic scale throughout a polymer host, forming a heterogeneous composite structure. This arrangement allows
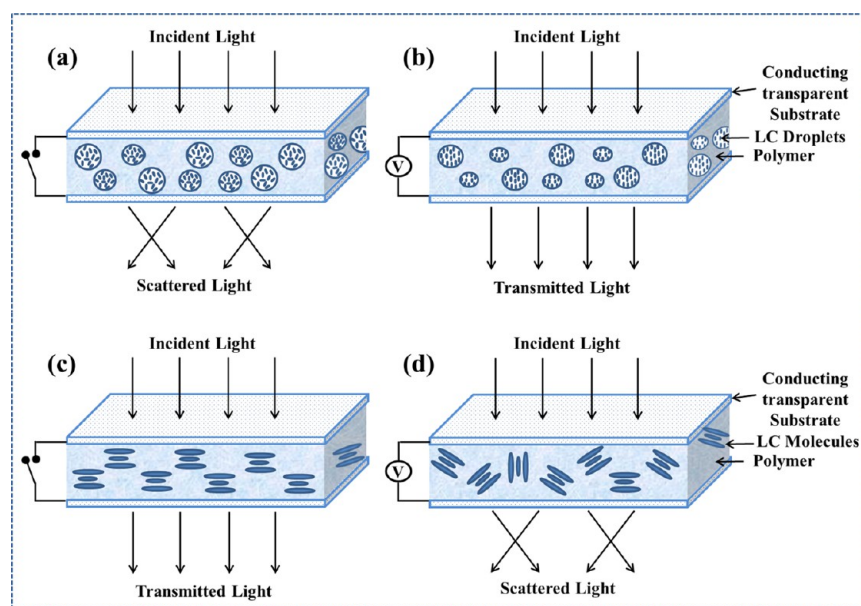
Figure 3. (a, b) Schematic representation of normal-mode PDLC in (a) OFF-state and (b) ON-state. (c, d) Schematic representation of reverse-mode PDLC in (c) OFF-state and (d) ON-state.

PDLCs to switch between transparent and opaque states by altering the alignment of liquid crystal molecules within the droplets, thereby controlling light transmission. By encasing micrometer-sized (or smaller) LC droplets in a continuous polymer matrix, PDLC films are created.[74,75] The concept of creating a random orientation of optically anisotropic LC droplets by embedding them in optically isotropic polymer matrix was first introduced by Fergason in 1984.[76] The thus-formed PDLC films have great technological importance, since they couple the peculiar anisotropic properties of LCs with the high mechanical and structural strength of polymers. PDLC films can alternate between their transparent and light-scattered states based on how LC molecules react to an external electric field and the degree of mismatch between the refractive indices of LC and polymer.[77] PDLCs are further classified as normal-mode PDLCs (NPDLCs) and reverse-mode PDLCs (RPDLCs).[74,78]

The working principle of NPDLCs devices can be understood as when the system is turned OFF, the majority of incident light is scattered because of the LC droplets' irregular orientation in the polymer matrix (Figure 3a) and the film appears to be in opaque state or the so-called light-scattered state. On the contrary, the refractive index (R.I.) of the polymer matches with that of the LC (ordinary (n_o) and extraordinary (n_e) R.I. for LCs with positive and negative birefringence, respectively) in the ON state. This matching of the two refractive indices results in the film being transparent upon the application of an electric field of appropriate strength, as depicted in Figure 3b. The LC birefringence affects the amount of light scattering in the voltage-OFF state of a normal-mode PDLC; the greater the birefringence, the greater the scattering efficiency. However, a continuous power supply is needed in case of NPDLCs for the light transmission state, which accounts for the high power consumption by the optoelectronic devices based on NPDLCs. On the other hand, contrary to the basic property of conventional NPDLCs, the RPDLC films are transparent in the OFF-state and become opaque upon applying an external electric field.[78,79] This situation is illustrated in Figure 3c and d. Althrough RPDLCs

have some drawbacks, like a difficult-to-use process, a poor yield, and the need for specialized LCs like cholesteric or dual-frequency LCs, they also have some unique qualities, like a higher contrast ratio than NPDLCs, good stability, superior mechanical qualities, and—most importantly—better environmental protection due to light transmission in the OFF-state. Because of this, RPDLCs are potential candidates for various optoelectronic uses.[78−80]

In addition, a brand-new class of PDLCs known as holographic PDLCs (HPDLCs) was created by fusing laser holography with traditional PDLCs. In these systems, phase separation by photopolymerization in PDLCs is triggered by a laser holographic interference light field. As a result, a periodic distribution-based refractive index-modulated grating is created in the polymer-rich region, and the LC-rich region corresponds to the laser interference's bright and dark stripes. It is usually referred to as HPDLC grating.[81,82] Since these systems have exceptional optical control properties, they are widely used in the field of optical-fiber switches and associated applications.[82−85] To maintain the comprehensive nature of the Review, further discussion in the subsequent sections will be limited to NPDLCs only.

2.1. Scattering Theory in PDLCs

The spatial variations of refractive indices of the materials account for the scattering in LCPCs.[86] The scattering in a PDLC is caused by the mismatch of R.I.'s of liquid crystals and polymers, while in the case of PSLCs the R.I. mismatch between the LC and polymer and that between LC domains both are the main causes of scattering. This section is dedicated to the qualitative discussion of this scattering in PDLCs.

During the propagation of light waves through a medium, a dipole moment is induced in each particle of the medium due to interaction with the electric field of the incident wave. As a consequence, each dipole oscillates with the frequency of incident wave, and these oscillating dipoles radiate light in all directions.[86] The net electric field at any point can be given as
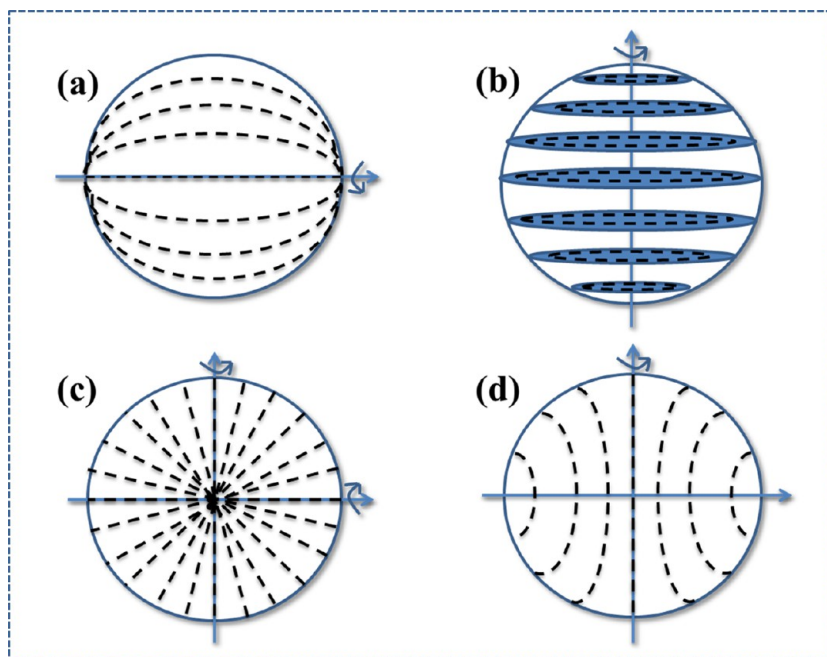
Figure 4. Different configurations of nematic droplets in PDLCs: (a) bipolar structure, (b) toroidal structure, (c) radial structure, and (d) axial structure.

the vector sum of field produced by all of the dipole radiators. For an incident light wave whose electric field is given as eq 1,

$$\vec{E}_{in}(\vec{r},\, t) = \vec{E}_o e^{(-i\vec{k}_o\cdot\vec{r}+i\omega t)} \tag{1}$$

the net scattered field can be represented as

$$\vec{E}_s(\vec{R},\, t) = -\frac{\pi}{\varepsilon_o R\lambda^2} V e^{(i\omega t - i\vec{k}'\cdot\vec{r})}\hat{k}' \times [\hat{k}' \times \{\vec{\alpha}(\vec{k}_s) \times \vec{E}_o\}] \tag{2}$$

where $\vec{\alpha}(\vec{k}_s) = \frac{1}{V}\int\vec{\alpha}(\vec{r})e^{i\vec{k}_s\cdot\vec{r}}d^3r$ denotes the Fourier component of polarizability $\vec{\alpha}$. V is the volume of the scattering medium, and $\vec{k}_o$ is the wave-vector of the incident light. For a spherical droplet of an isotropic medium with refractive index n and radius a, surrounded by an isotropic medium of refractive index n_o, the scattered light can be mathematically expressed using eq 3 given below, where the integrals can be calculated within the limits $[0,\, \pi/2]$ and $[\pi,\, \pi/2]$ for forward and backward scattering, respectively.

$$\sigma = \pi a^2 (2\overline{n}\Delta n)^2 \int \frac{(\cos^2\theta + 1)}{64A^2}\left\{\frac{\sin[2A\sin(\theta/2)] - 2A\sin(\theta/2)\cos[2A\sin(\theta/2)]}{\sin^3(\theta/2)}\right\}^2 \sin\theta d\theta \tag{3}$$

The above calculations can also be extended for LCs by taking their dielectric tensor into consideration.[87,88] However, it is important to mention that the formulations given above based on Rayleigh−Gans scattering make use of two assumptions: (1) $|n/n_o - 1| \ll 1$, i.e., the refraction at the droplet interface is negligible, and (2) $2k_oa|n - n_o| \ll 1$ and $\sigma \ll 1$, which means the light intensity at any point inside the medium is the same and multiple scattering does not occur inside the droplet. However, in the case of PDLCs, the droplet diameter is about 1 μm, and for visible light $|n - n_o| \sim 0.2$, which means that $2k_oa|n - n_o| > 1$. Thus, for PDLC systems, the Rayleigh−Gans scattering theory does not hold true. The scattering through PDLC devices can be explained in a better way using anomalous diffraction theory,[89,90] which is based on the following assumptions: (1) $|n/n_o - 1| \ll 1$, i.e., the refraction at the droplet interface is negligible, and (2) $k_oa \gg 1$, which means a light ray can be retraced. As per the assumptions of this theory, the light wave, incident on a LC droplet, passes through the droplet without any scattering, but the phase in the wave beyond the droplet gets modified by the anisotropic LC. According to Huygen's principle, all the points on this emergent wave emit secondary spherical waves, and the

scattered field is the sum of all of these waves. Multiple scattering can also take place if there is a sufficient number of scattering droplets in the medium, and it tends to make the scattering profile broader.[91,92]

2.2. Droplet Configurations in PDLCs

Though different mesophases, such as nematic, cholesteric, smectic-A, smectic-C*, ferroelectric, and antiferroelectric LC phases, are used in PDLC devices, the most commonly employed one is the nematic phase.[60,93−96] Therefore, this section discusses the different droplet configurations of nematic liquid crystals (NLCs) in the polymer matrix. The orientation of the director in a nematic droplet is affected by a number of factors such as droplet size, shape, anchoring conditions on the droplet surface, externally applied electric field, elastic constants of the host LC, etc.

For tangential anchoring conditions, generally two types of droplets are observed; one is the *bipolar droplet* structure shown in Figure 4a. In these droplets, the bipolar axis defines the axis of rotational symmetry, and the unit vector along that axis denotes the director.[97−99] Two point defects are seen at the extremities of the diameter along the bipolar axis when
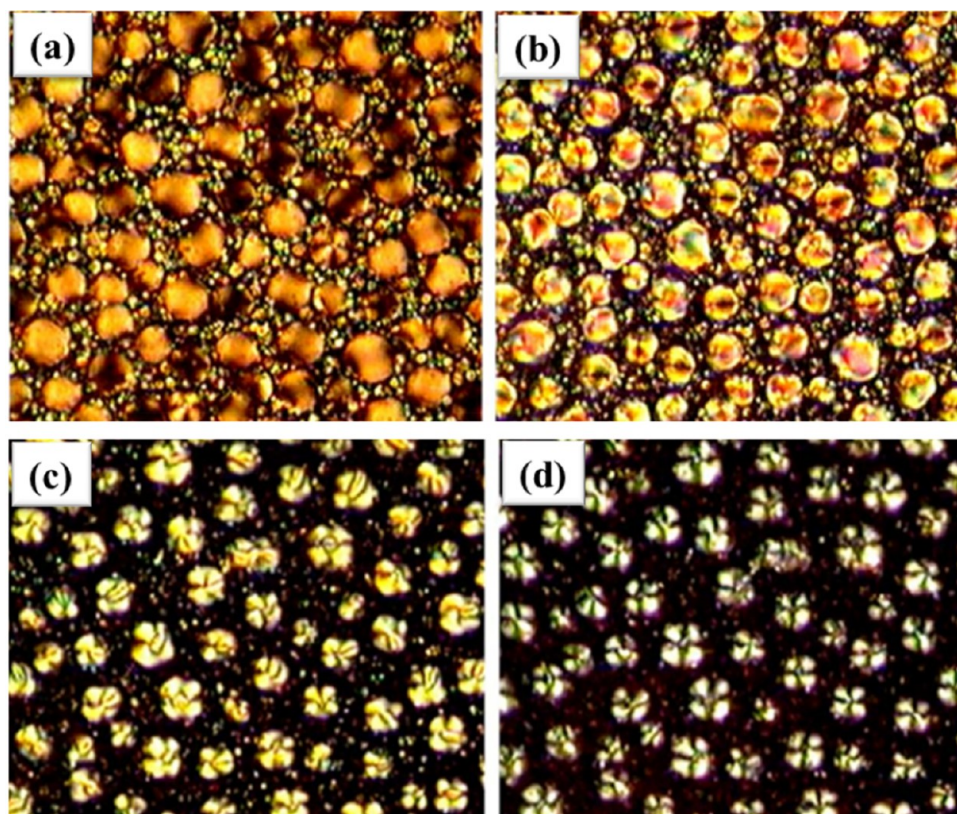
Figure 5. (a−d) Transition of droplet configuration from (a) bipolar (in the absence of an electric field) to (d) radial (at ∼25 V_{p-p}) configuration with increasing electric field. Reproduced with permission from ref 108. Copyright 2004 Elsevier.

strong anchoring conditions are met. Along the diameter of the droplets, the director is parallel to the bipolar axis, while it is tangential to the circle along the circumference of the droplets. The orientation of the director at all of the other places is such that it minimizes the total energy of the system. The other droplet structure observed in case of tangential anchoring is the *toroidal droplet* structure illustrated in Figure 4b. In this instance, a line defect appears along the diameter, and rotational symmetry surrounds the defect as the director aligns in concentric circles on planes perpendicular to the diameter.[100] However, the occurrence of toroidal droplets is quite rare because of the fact that this droplet structure exists when the bend elastic constant is smaller than the splay elastic constant of the LC, which is not generally the case in most of the LCs. Nevertheless, there are few reports where the existence of toroidal droplets in PDLCs has been found.[101,102]

On the other hand, two different kinds of droplets, i.e., axial and radial droplets, can be observed when the anchoring conditions are perpendicular. The configuration where a point defect exists in the droplet center and the director is positioned along the radial direction through the entire droplet is called a radial droplet structure, as depicted in Figure 4c. In this case, the rotational symmetry exists around any diameter of the droplet, and it has been observed through polarized optical microscopy (POM) that the POM image does not change upon rotating the microscope stage. In the radial droplets, only splay elastic deformation exists, and there is a small region at the center of the droplet where the director is parallel to any one of the polarizers.[103,104] This region appears dark in the POM image. In contrast to radial droplets, there is a line defect along the equator in axial droplets, as shown in Figure 4d.

Rotational symmetry exists around the diameter perpendicular to the plane of the equator. The radial and axial droplets appear to be almost same through POM, with the only difference being that the dark cross at the center is wider in case of axial droplets.[98,105] It has previously been noted that a spontaneous transition from radial to axial ordering occurs when the LC droplet size falls below a certain value.[103] Previous research has also shown that the application of an external electric field causes an LC droplet to undergo a transition from one configuration to the other. The size of the LC droplets in the PDLC systems determines the strength of the field needed to cause this transition.[103,106−108] One such change has been reported by P. Malik et al., who observed a transition of the LC droplet from a bipolar structure (in the absence of the field) to a radial configuration at the center at sufficiently high field (∼25 V_{p-p}), as illustrated in Figure 5.[108]

Besides the aforementioned droplet structures, there are some other configurations that also exist under a given set of conditions, such as the formation of twisted bipolar droplets upon the reduction of splay and bend elastic energy due to the inclusion of twist deformation, removal of point defects in the radial droplets from the center for the minimization of total free energy, etc.[109,110]

3. MECHANISMS OF PREPARING PDLCs

Polymer-dispersed liquid crystals refer to a specific form of liquid crystal technology that utilizes microscopic liquid crystal droplets scattered throughout a polymer matrix. These droplets can be manipulated to change the orientation of the liquid crystals, resulting in a device that is capable of fast response times and high contrast ratios. The fabrication of
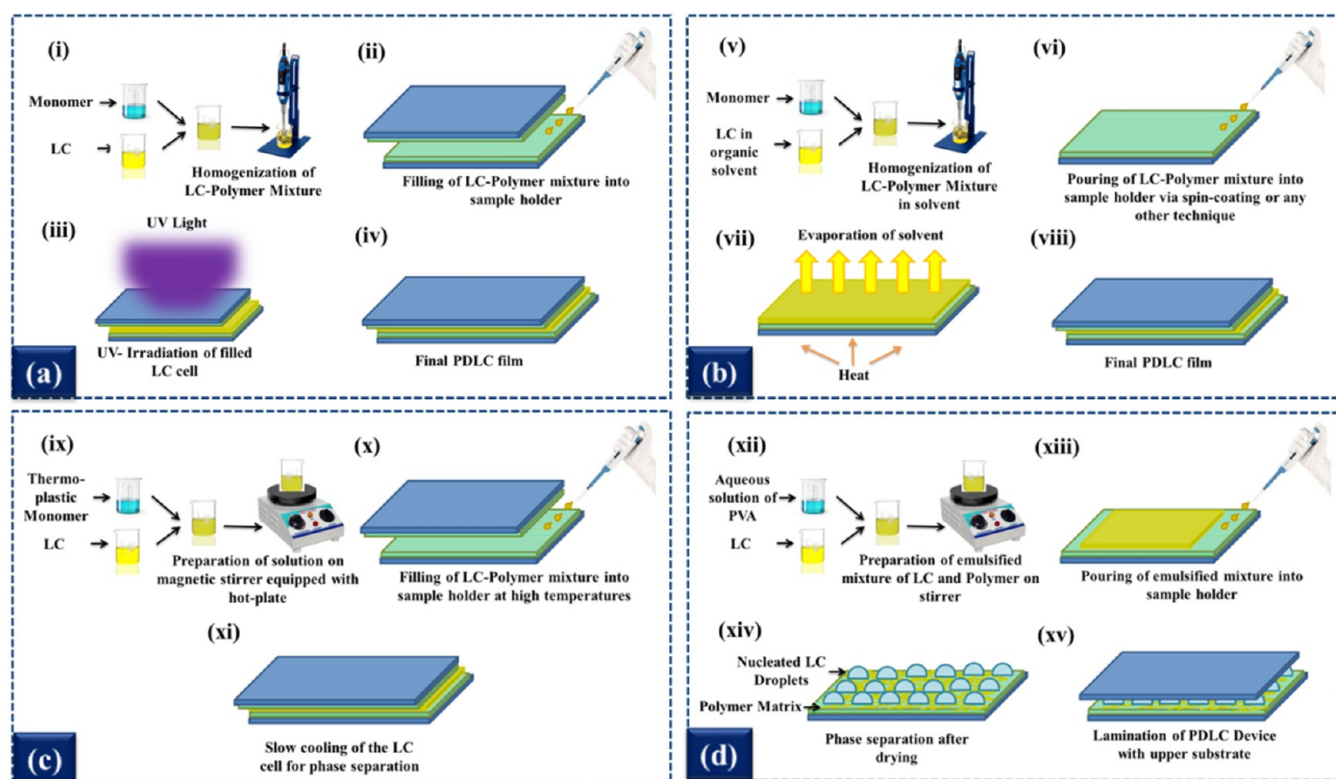
Figure 6. Schematic stepwise illustrations of different techniques used for creating phase separation in a PDLC system: (a) polymerization-induced phase separation (PIPS), (b) solution-induced phase separation (SIPS), (c) temperature-induced phase separation (TIPS), and (d) encapsulation.

PDLCs involves precise control over the dispersal and alignment of liquid crystal droplets within the polymer matrix. Fabrication techniques for PDLCs encompass a range of approaches tailored to achieve specific droplet sizes and distributions. Initially, a homogeneous isotropic solution of LC and prepolymer (or monomer) is prepared, and a variety of methods can be adopted in order to persuade the formation of nucleated LC droplets in the polymer matrix after phase separation. The technique employed for phase separation plays a key role in determining the performance and attributes of the prepared PDLC devices. It has been experimentally verified that the morphological and physical attributes of LCPCs depend effectively on the chemical nature of LCs/polymers and the technique of phase separation, along with its extent, employed in the formation of these composites. Besides that, there is an additional significant influence of the surface anchoring conditions on the phase separation dynamics. In the conventional PDLC cells without a polyimide (PI) layer or with a PI layer (without rubbing), the LC droplets flow and coalesce with the other droplets after phase separation to form larger droplets; thus, the size distribution in such PDLC cells is not uniform. On the contrary, in the twisted-nematic (TN) cells and homogeneously aligned (HA) cells, the strong anchoring force of the alignment layers prevents the coalescence of droplets, which results in the very uniform surface morphology of the PDLC cells with the formation of smaller LC droplets after phase separation.[111]

Generally, there are four commonly employed conventional routines of crafting phase separation in LCPCs: polymerization-induced phase separation (PIPS), solution-induced phase separation (SIPS), temperature-induced phase separation (TIPS) and encapsulation. The schematic illustration of each of the techniques is presented in Figure 6. In the PIPS technique, a homogeneous solution of LC and monomers (or oligomers) with acrylate or methyl acrylate end groups (in addition to a suitable photoinitiator) fills a typical capacitor-type LC cell. The sample holder is irradiated with ultraviolet light of suitable energy and intensity for a stipulated time duration (see Figure 6a). The incident radiation induces the process of polymerization, and the growing polymeric chains separate the LC droplets in the form of isolated islands.[112−114] In the SIPS method of phase separation, the mixture of LC and polymer is prepared in any appropriate organic solvent. A suitable technique is adopted to pour the solution onto an optically transparent and conducting substrate (see Figure 6b). Phase separation after polymerization occurs upon heating of the substrate and evaporation of the solvent, and the thus-prepared film is covered with another substrate.[115] The rate of heating/cooling tailors the morphology of the PDLC system. Thermoplastic polymers are found to be suitable for the fabrication of PDLC films using the TIPS technique. The solution of such polymers and LCs is prepared at high temperature to form a homogeneous and clear solution, which is then filled in LC cells, as illustrated in Figure 6c. During the cooling cycle, the phase separation occurs between the two entities. Despite being easy to perform, this method is less preferred because the physical properties of the thus-formed PDLC films are not reproducible and such films do not offer fair electro-optical properties. In contrast to the methods of phase separation discussed above, the encapsulation or emulsion-based method involves the preparation of an inhomogeneous solution of LC and polymer. To begin with, the host LC is mixed in an aqueous solution of polymer such as poly(vinyl alcohol) (PVA) by rapid stirring as an emulsion.

This emulsified mixture is deposited on conducting electrodes and dried. The nucleated LC droplets (see Figure 6d) surrounded by the solid polymer are produced on the substrates, and the dimensions of these droplets are controlled by stirring speed and time.[116−118] Lamination of another conductive substrate onto this film finally forms the final PDLC device.

Each approach offers unique advantages in terms of droplet size distribution, scalability, and compatibility with different polymer systems. The detailed advantages and disadvantages of these procedures are listed in Table 1.

Apart from the aforementioned conventional techniques, some novel nonconventional routines for the preparation and fabrication of PDLC devices, such as microfluidics,[119] coaxial electrospinning,[120] and aerosol jet printing,[121] have also been followed in past decades. Out of all of these methods, a standard approach that is commercially adopted to achieve phase separation during the production of PDLCs as well as PSLCs is PIPS. Though this process requires high precision and the consideration of all the governing factors in the involved chemical reaction, the easy-to-conduct manipulation of this technique and the adequate morphologies of the finally prepared PDLC make it the most appropriate choice.[122] In this process, the intensity and duration of UV illumination determine the extent of polymerization in the heterogeneous mixture of polymer and LC[123,124] and thus determines the morphology as well as various electro-optical properties, which are also affected by other external stimuli like the anisotropy and birefringence of the LC involved, the temperature of the surroundings, the applied electric field intensity, and others. The concentration of photoinitiator also tends to affect the phase separation process and hence controls the morphological and electro-optical performance of the thus-formed PDLC systems.[125]

However, using polymers as additives to the LC matrix provides rigidity to the system and thereby increases its threshold voltage and operating voltage, which is not desirable for practical purposes.[126,127] To overcome this problem, different researchers have added a variety of dopants, such as quantum dots, metallic and nonmetallic nanoparticles of different sizes and properties, dyes, etc., to enhance the operating parameters of the composites and make them a suitable choice for device applications.[128−134] This will be discussed in a subsequent section of this Review.

4. MATERIALS USED IN PDLC SYSTEMS

For commercial purposes, a PDLC device must be capable of demonstrating superior optical switching characteristics with a smaller operating voltage and optimally better response time attributes. For controlling these elements, a careful choice of raw materials and the addition of suitable dopants have been performed and analyzed by different research groups in recent years. The same have been classified and discussed comprehensively in the subsequent subsections.

4.1. Types of Liquid Crystals Used

Different LCs have been used, in recent decades, to explore the effect of different mesophase configurations on the performance of PDLCs for the sake of technical utility. Among different mesophases, the nematic LCs (NLCs) have been used the most because of their large optical anisotropy and adaptable applications.[135] Out of all of the available NLCs and polymers, the combination of E7/NOA65 is the most explored

Table 1. Advantages and Disadvantages of different conventional techniques of phase separation

s. no.	parameters	TIPS	PIPS	SIPS	encapsulation
1	cause of phase separation	temperature variation	UV irradiation for stipulated time-span	solvent evaporation due to temperature variation	rate of drying of LC–polymer emulsion
2	surface morphology of PDLC (size of microdroplets)	rate of cooling/heating dependent (any abrupt change in this rate would lead to distorted morphology)	UV curing time and intensity	rate of extraction of solvent which, in turn, depends upon the rate of heating/cooling	speed and duration of stirring while emulsification of polymer–LC composite.
3	advantages	simplicity	low activation energy, broader working temperature range, good control over final properties	this technique provides a scope to alter the dimensions and configurations of LC droplets even after one cycle of phase separation with the help of repeated heat/cool cycles	since LC is insoluble in aqueous solutions, equilibrium phase separation is easily achieved using this technique, no polymer plasticization observed
4	disadvantages	reduced thermal stability of devices; less stable surface morphology due to temperature dependence	curing conditions and choice of materials play key role, which is typical to optimize	solvent recycling requires additional equipment that increases the expense and complexity; EO performance degraded because of thermoplastic resin polymers; less stable surface morphology due to temperature dependence	significant change in the volume of the film due to water evaporation; deformations in droplet structure; lack of appropriate polymers for this technique
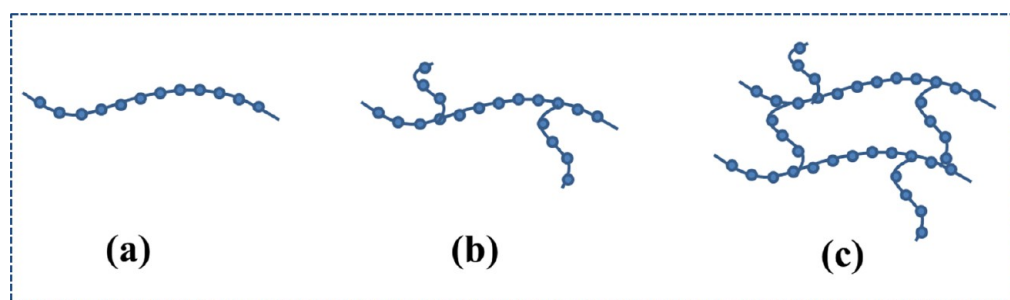
Figure 7. Schematic illustrations of different polymer structures: (a) linear, (b) branched, and (c) cross-linked polymer structures.

one. This is because the R.I. of polymer NOA65 (1.524) matches well with the ordinary R.I. (n_o = 1.525) of the LC mixture E7 and thus provides a good contrast between the hazy (or opaque) and transparent states of the films. The versatility of cholesteric LCs (CLCs) and smectic phases in the PDLC systems has been widely explored.[94,110,136,137] A bistable smectic A (SmA) LC mixture was prepared by mixing 8CB, 10CB, 12CB, 5OCB, and CTAB (for ionic doping), and the performance of the PDLC film based on this LC was analyzed by Y. Lu et al. in a recent study,[62] where they optimized the performance of the film using monomer concentration as well as functionality, curing temperature, and curing intensity. Similar studies have been performed on polystyrene (PS)/10CB- and PS/12CB-based PDLC composites to study the phase transitions in the composites, and relevant theory has been provided.[138]

Ferroelectric liquid crystals (FLCs) have also been explored for their potential applications in PDLC systems.[60] The effect of polymer concentration on the performance parameters of polymer-dispersed FLCs has been studied by P. Malik et al., who observed a decrease in FLC droplet size with increasing polymer content that hinders the helicoidal motion of FLC, thereby influencing the dielectric property, conductivity, and higher energy band gap of the system.[139−141] The group also reported the enhancement of the spontaneous polarization, dielectric strength, and anchoring energy coefficients of the polymer-dispersed ferroelectric liquid crystal (PDFLCs) on account of dispersion of different nanomaterials such as ZnO nanoparticles and porous carbon nanoparticles (PCNPs).[132,142]

Different terminal groups on the mesogenic units also play an important role in determining the performance parameters of PDLC films. As per the study conducted by J. Xu. et al.,[143] the substituted fluorinated mesogenic units (containing ≥10 wt % fluorine component) exhibit low driving voltages at low temperatures but poor contrast at high temperatures, whereas the cyano-LC molecules in PDLC films show excellent contrast at higher temperatures as well.

## 4.2. Description of Polymer Utilized

To achieve better contrasting modes (light scattering and light transmitting modes) in a PDLC-based device, the material choice plays a crucial role. While choosing appropriate polymers, it is kept in mind that the R.I. of the polymer must match with either of the two refractive indices (n_e or n_o) of the used LC so that the resulting PDLC films can exhibit a controllable scattering effect. For this purpose, different polymers have also been explored in a wide range of LCs; however, before analyzing the effect of different polymers on the performance of PDLC devices, it is important to understand the different polymer structures and the corre-

sponding variations in their chemistry caused by their structural changes. This is explained in the following subsections.

4.2.1. Polymer Chemistry. We are already aware of the fact that polymers are composed of very large molecules called macromolecules, which are multiples of simpler repetitive units known as monomers. In the case of sufficiently regular structures, caused by a lack of variation in the monomer (as in case of many homopolymers), the polymeric chains tend to form ordered crystallites. Therefore, polymers can be considered to be consisted of small crystalline domains connected by amorphous regions. The amount of these crystalline and amorphous domains plays a decisive role in the determination of the polymer structure and, hence, its properties. Polymers having crystalline regions exhibit a melting transition temperature (T_m) and a second-order phase transition at the glass transition temperature (T_g), with $T_g < T_m$. At T_g, a slow change in the mechanical properties of the polymers is observed, as this transition is a consequence of the sudden onset of increased molecular motion of the polymer chain above this characteristic temperature. Most of the polymers used in PDLC devices absorb the LC (indication of good solubility of the LC in the polymer), and therefore both the T_g and T_m of the polymer are lowered by a process called plasticization. It is likely that the polymers in PDLC systems have strongly suppressed T_g and T_m values. However, an exception is found when the polymer itself is mesogenic (as in case of LC elastomers). Such systems include main-chain or side-chain polymers as well as highly cross-linked mesogenic diacrylate materials, but further discussion on these systems is out of the scope of this Review.

Numerous monomers connect and interlink together in several ways to form a variety of polymer structures. The resulting polymer chains can be linear, branched, or cross-linked, where different linear chains are connected to each other as shown in Figure 7.

Linear and branched polymers are generally soluble in different solvents. On the contrary, cross-linked polymers have very high molecular weights and therefore do not get dissolved in solvents. In fact, they maintain their network structure in solvents as they swell after absorbing solvents. Thus, they are tough, durable, and resist any mechanical deformations. For these reasons, cross-linked polymers are preferred for *emulsion-based* and *polymerization-induced* phase separation techniques. In contrast, the linear polymers can easily be deformed by the slippage of polymer chains or by variation in the crystallite structure. Therefore, *solvent-induced* and *temperature-induced* phase separation techniques make use of linear and branched polymers.[144]
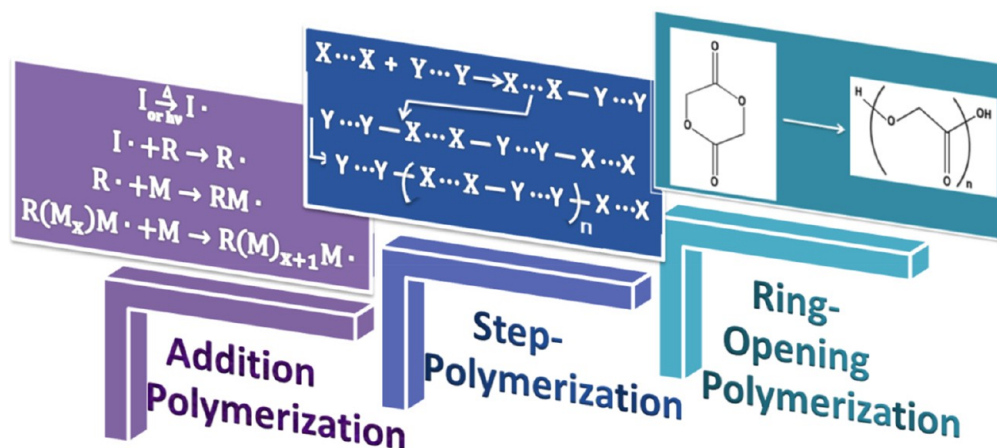
Figure 8. Different polymerization reactions and schematics of their related kinetic schemes. (a) Addition polymerization, in which a free radical (I•) is formed due to thermal or photoinitiated activation of the initiator (I). This free radical reacts with the species R and activates it to (R•), which further combines with the monomer M and causes rapid chain growth. (b) Step-polymerization (schematic for the reaction between monomers with reactive groups X and Y). (c) Ring-opening polymerization (reaction scheme for conversion of glycolide to polyglycolide).
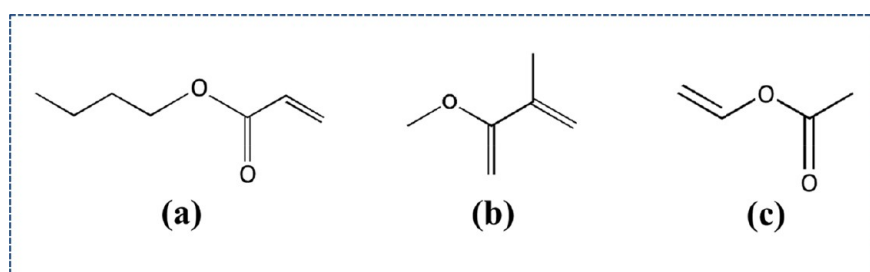
Figure 9. Molecular structures of some monomers that undergo addition polymerization and are commonly employed in PDLC films: (a) *n*-butyl acrylate, (b) methyl methacrylate, and (c) vinyl acetate. The first two are generally used in the PIPS process, while the third one acts as a precursor of poly(vinyl alcohol) for emulsion-based systems.

4.2.2. Polymers in PDLCs. We have seen in the previous section that different structures exist for a monomer, and the fundamental requirement for a molecule to act as a monomer is its ability to connect with other molecules in a repetitive manner. Three basic strategies can be adopted by a molecule to achieve such multifunctional character: (i) addition polymerization (or free-radical polymerization), which involves the opening and activation of molecular double bonds through external stimulus (such as heat or light) for linking with other similar bonds via either cationic, anionic, or free radical reactions; (ii) step-polymerization, where each reactive species can couple to only one other monomer; and (iii) ring-opening polymerization (refer to Figure 8).

In addition to polymerization, LCs are mixed with the monomer prior to reaction in order to form a polymerized PDLC film. The system is exposed to either heat or light for the reaction to be initiated to form free radicals. Generally, a suitable initiator is used to facilitate the creation of free radicals in the composite system upon exposure to external stimuli. While many different types of unsaturated species can be used in addition polymerization, the most commonly used are those derived from acrylate, methacrylate, or vinyl families.[145] The molecular structures of these monomers are shown in Figure 9. The substituents attached to these reactive groups can be varied, possessing a range of polarities, containing other reactive species, or being liquid crystalline by themselves. The use of multifunctional acrylates or vinyl groups (i.e., more than

one reactive group per monomer) allows for cross-linking to occur between them.[146,147]

Norland Optical Adhesive 65 (NOA65) is one of the most employed commercially available photocurable polymers for these purposes because its R.I. (~1.5) is close to the n_o value of most of the commercially available LC mixtures.[63] It is a mix of an acrylate monomer and a mercaptan ester radical manufactured by Norland Products Inc. It is a liquid prepolymer that facilitates the formation of a photopolymer upon UV irradiation. It is preferred generally because using NOA65 eliminates premixing, drying, and heat curing operations common to other optical adhesives, and the polymer exhibits a very fast curing time. Due to its better flexibility, it exhibits fairly good electro-optical properties when coupled with LCs for the formation of PDLC films.[148−150] The inclusion of methacrylate monomers tends to enhance the electro-optical (EO) properties of PDLC films more than the acrylate monomers.[151,152] It has been observed that fluorinated monomers also boost the EO performance of the PDLC devices.[153] Furthermore, it was reported recently that hydroxylated acrylate monomers tend to enhance the adhesion strength of PDLC films significantly, without any compromise with their high EO properties.[154−156] Besides that, increasing cross-linking agent also tends to reduce the LC droplet size, resulting in low operating voltage requirements.[157]

In contrast to addition polymerization, step-polymerization makes use of multifunctional reactants for cross-linking purposes. However, this strategy is generally less preferable

for PDLC systems because these reactions are followed by the release of a small molecule (such as water) as a byproduct, and it will be a difficult task for the PDLC film to get rid of these byproducts.[158]

The ring-opening polymerization reaction involves the reactants containing a cyclic structure as observed in the case of the epoxide group (three-membered ring with an oxygen atom as one of the members, see Figure 8). The reactant is attacked by any nucleophilic group (such as thiol group) so that its ring is opened for cross-linking.[159,160] Optimization of the structure of curable epoxy polymers can help in the regulation of EO properties of PDLC systems.[161,162]

Increasing the functionality of thiol monomers tends to increase both threshold voltage (V_{th}) and saturation voltage (V_{sat}),[163−165] but this rate of increment of V_{sat} is generally low in case of increasing the functionality of acrylate monomers. Both V_{th} and V_{sat} decrease evidently on increasing the chain length of flexible cross-linker used during PDLC formation.[163] Chen et al.[166] probed the mechanical and electro-optical attributes of PDLC films upon the integration of rigid monomers and found that the optimization of polymer, LC, and dopant concentrations with the polymerization process results in reduced driving voltage, enhanced contrast ratio, and faster response time, making these films suitable for novel smart optical materials. Not long ago, a novel approach for improving the electro-optical attributes of PDLC films was reported by implanting the polyhedral oligomeric silsesquioxane (POSS) microstructure into the polymer matrix. The polymer meshes broaden with the increasing content of POSS microstructures, and the anchoring effect gets reduced, which serves as the driving force for optimized electro-optical performance.[167]

Recently, Y. Wu proposed the fabrication of a triple-layer PDLC film having appreciable application value in the field of progressing driving display.[168] Three UV curing agents (UV6301, UV65N, and UV64-5) with two different functional cross-linkers (PEGDA400 and PEGDA1000) were mixed in NLC SLC1717 for this purpose with a small quantity of photoinitiator Irgacure 651. The fabricated PDLC film displayed a progressive drive function in which the transmittance can be controlled by applying low voltages only. It displayed around 31% and 56% reduction in the threshold and saturation voltage, respectively, with a 20% reduction in OFF-state response time and 21% increase in contrast ratio. Another similar comparative study was recently conducted by N. Balenko et al., where the influence of three different polymers (PDMS, PU, and plasticized PVA) on the mechano-optical response of a polymer-dispersed cholesteric LC were studied and the PU-based composites were found to be the most promising for application purposes.[169] The effect of different polymers on the dielectric and electro-optical properties of PDLC composites has been studied by different research groups, and the same is tabulated in Table 2. For molecular structures of different LCs and polymers utilized in the PDLC systems, please refer to Supporting Information (SI) Figures S1 and S2, respectively.

From Table 2, we see that the optimization of superior EO properties can be achieved by using a suitable monomer or oligomer for the preparation of PDLC films. Also, it has been observed that the replacement of conventional non-liquid-crystalline monomers in PDLC films with acrylate-based LC monomers provides a good control over the morphological and EO behavior of the system.[173] Such systems also exhibit

Table 2. Effect of Different Polymers on the Dielectric and Electro-Optical Properties of LC–Polymer Composites in the PDLC Systems

LC	polymer	results	refs
SLC 1717	pentaerythritol tetrakis (2-mercaptoacetate) (4SH), trimethylolpropane triacrylate (TMPTA), and polyethylene glycol diacrylate (PEGDA 600)	driving voltage ↓ (24 V), high contrast ratio ↑ (97), response time ↓ (<8 ms)	M. Saeed et al.[163]
5CB (49.5 wt %)	polyvinyl acetate (PVAc) (49.5 wt %); metal NPs: AgNPs (globular, 150 nm), CuNPs (globular, 150 nm), SiNPs (spherical, 30–50 nm); dielectric NPs: SiO$_2$ (spherical, 30–50 nm); composite NPs: TaSi$_2$/Si, Ag/Si (1 wt %)	dielectric anisotropy $\Delta\varepsilon$ ↑, response time ↓	S. V. Kalashnikov et al.[170]
ZLI-3239	poly(dimethylsiloxanecoalkylmethylsiloxane) (PDMS); silica NPs: silica NPs (5–15 nm)	electrical tuning of photoluminescence achieved, better optical stability and improved off-state scattering	R. Kumar et al.[171]
C7	triethylene glycol diacrylate (TEGDA), trimethylolpropane diallyl ether (TMPDE), trimethylolpropane tris(3-mercaptopropionate) (TMPTMP), and NOA65; AR1 (red) and AB4 (blue) dichroic dyes	fractal-structured geometry in droplets, relative transmission ↑, response time ↓, power consumption ↓	S. Kumar et al.[172]

exceptional bending resistance and flexibility with outstanding EO properties.[174] Furthermore, it is proven that the length of the alkyl chain of acrylate monomers affects the contrast ratio of PDLC systems significantly, and the inclusion of branched chains can also help in the reduction of driving voltage.[175]

Ferroelectric poly(vinylidene fluoride) (PVDF) polymer has also appeared as a viable prospect for LC device design. As reports suggest, several interesting optical and electro-optical effects resulted from the interaction between the LCs and the mechanically rubbed PVDF layers. Afterward, it was observed that the copolymer of PVDF and trifluoroethylene (P(VDF-TrFE)) may crystallize in the ferroelectric phase during solidification from solution. Thus, replacing the homopolymer PVDF with this copolymer may lead to better EO properties of PDLC systems, as confirmed experimentally.[176] It was shown how significantly the remnant polarization of P(VDF-TrFE) copolymer-based PDLCs affected the samples.[176] When piezoelectric and electro-optical effects combine, the electric field produced by the mechanical stress alters the way the PDLCs transmit.[177]

4.3. Discussion of Additives and Dopants

A large variety of organic and inorganic additives have been doped in PDLC systems in order to enhance their performance parameters. Intriguing electronic, optical, and magnetic properties are exhibited by inorganic nanoparticles (NPs) depending on their shape, size, composition, and concentration in the system. For this purpose, different kinds of nano-particles, such as plasmonic nanoparticles, noble metal-based nanoparticles, ferroelectric and ferromagnetic nanoparticles, etc., were added to PDLC systems to modulate their optical and electro-optical properties.[61,128,178−184] The size of nano-particles or quantum dots (QDs) doped into LCPCs significantly affects the properties of thus-formed PDLC devices. Nanoparticles (NPs) or QDs that are larger in dimension increase the amount of scattered light and thereby improve the contrast ratio of the PDLC system between the hazy and transparent states. The addition of smaller NPs or QDs adjusts the effective refractive index matching of the composite system. This gives the PDLC systems some special properties such as enhanced luminescent attributes, better EO performance, and many others. The remnant polarization of ferroelectric NPs effectively perturbs the LC alignment, decreasing the operation voltage and response time of the PDLCs. Gold NP (AuNP) doped PDLCs, as examined by THz time domain polarization spectroscopy, exhibit a faster and more uniform relaxation response to a high-frequency electric field, making them a suitable option for tunable THz LC phase and polarization devices.[185] The high electrical conductivity of graphene oxide (GO) leads to the production of a higher internal electric field in a PDLC system, yielding superior photorefractive and third-order nonlinear optical properties.[186] Apart from being an excellent doping agent, GO has also been proven as a great alternative as a transparent electrode in PDLC films in place of the highly expensive indium tin oxide (ITO) electrodes owing to the low resistivity, high chemical stability, fairly high optical transmittance, and mechanical strength of the GO layer.[187−189] The doping effect of different cation exchange capacity (CEC) clays on the morphological and electro-optical properties of E7/NOA65-based PDLC films have been studied by T.-Y. Tsai et al.[190] They used two different natural clays, viz., CL120 and CL42, as inorganic nanofillers in different concentrations and

observed a huge reduction in the driving voltage and dynamic response time of the PDLC films. The comparative analysis of organic and inorganic dopants influencing the optical, dielectric, and electro-optical performance of PDLCs is provided in Table 3.

5. APPLICATIONS OF PDLCs

Owing to their electrically switchable properties, PDLC composites have garnered enormous interest in the fields of smart windows, optical shutters, switchable glazing, organic photorefractives, polymer gravel lenses, and many others.[64,200,207] Huge success has been achieved in the fabrication of PDLC-based devices for commercial purposes. The development and creation of innovative modes and performance regulation have always been the main goals of PDLC research and manufacturing, notwithstanding the commercialization of certain associated products. There are some certain shortcomings inherent with PDLC systems, such as higher operating voltage, low UV-shielding, lack of flexibility due to ITO-based electrode requirements, smaller working temperature range, complexity in designing large-scale devices, etc. Several efforts have been made to overcome these drawbacks and enhance the technical utility of these materials. The subsequent sections discuss the development of PDLCs in different fields.

5.1. Organic Photorefractives

Through variation of the microstructures of polymer−LC composites, the unique characteristics of PDLC and PSLC systems can be modified. These systems can be used to prepare tunable photorefractives or flexible photovoltaic films with the potential for large-scale manufacturing in future technologies. One such technique was proposed by H. Yang[208] by combining the advantages of both PDLCs and PSLCs. They proposed a novel coexistent system of polymer-dispersed and stabilized LCs prepared using NLC monomers (TMHA and BDDA), LC monomer (C6M), and SmA-N*LC [SmA LC (8CB/10CB/12CB/8OCB = 19.7:8.0:13.0:59.2)/SLC 1717/ chiral dopant (S811) = 69:18:13] and photoinitiator (I651) in different compositions. The desired homeotropically aligned polymer network (HAPN) was achieved within the LC droplets after phase separation for the film containing (TMHA+BDDA)/C6M/(SmA-N*LC) in the ratio of (16.0 + 4.0)/3.0/77.0 wt %. The thin flexible film prepared by such systems exhibited reversible transmittance within transparent and opaque states via thermal controlling. Figure 10a−f show the schematic illustrations of the film, before and after UV curing, at different stages to achieve the final HAPN network illustrated in Figure 10g. The images of transparent and light-scattering states are displayed in Figure 10i and j, respectively, and the film was reported to display a strong shearing strength.

PDLCs have potential use in the development of flexible LC gratings. It was previously reported that PDLC composites filled in a flexible cell composed of ITO-PET substrates exhibit very low driving and saturation voltages (0.8 and 12 V for 1D; 2.5 and 16.5 V for 2D) and modulated grating diffraction order with faster response.[209]

5.2. Optical Shutters and Switchable Glazing

A switchable glazing (or window) that switches between transparent and opaque states upon the application and removal of electric fields has been one of the most common applications of PDLC devices used for energy-efficient purposes. Dye-doped PDLCs generally exhibit a high contrast

Table 3. Comprehensive Analysis of Different Dopants Affecting the Performance Parameters of the PDLC Systems

liquid crystal	polymer	inorganic/organic dopant details	phase separation technique	major findings[a]	ref
SCB (30 wt %)	heat-curable epoxy resins, polypropylene glycol diglycidyl ether (PPGDE; 19 wt %) and ethylene glycol diglycidyl ether (EGDE; 36 wt %), hardener (DETA; 15 wt %)	BaTiO₃ (spherical; diameter 5–15 nm; 0.25, 0.33, 0.40, 0.47, 0.55 wt %)	temperature-induced phase separation (TIPS)	off-state transmittance (T_{OFF}) ↓ 0.63%; on-state transmittance T_{ON} ↑ 79.9%; V_{Th} ↓; V_{Sat} ↓; contrast ratio ↑ 55×; τ_{rise} ↓; τ_{fall} ↑ (optimum results for 0.40 wt % NPs)	A. Kumari et al.[180]
E7 (50%)	NOA65 (50%)	BaTiO₃ (30–50 nm) ZnO (60–80 nm) both NPs were taken in amounts of 0.2, 0.4, 0.6, 0.8, and 1.0 wt %	UV curing (PIPS); 160 W; 15 min	V_{Th} ↓ 85%; V_{Sat} ↓ 41%; τ_{rise} ↓; τ_{fall} ↓ (optimum results for 0.8 wt % BaTiO₃ NPs); peizo-tribo effect was observed; energy generation application was proposed	V. N. John et al.[191]
E7	PEGDA 400, hexyl acrylate (HA), catalyst DMAP, PETMP	BaTiO₃ (0.02, 0.05, 0.1, 0.2, 0.3, 0.5 wt %)	heat curing at 80 °C	off-state transmittance (T_{OFF}) ↑; on-state transmittance T_{ON} ↓; V_{Th} ↓; contrast ratio ↓ (optimum results for 0.2 wt % NPs)	T. He et al.[192]
E7 (40%, 50%)	NOA65 (60%, 50%)	BaTiO₃ (diameter 8 nm, 20 nm, 2 μm); 0.3 vol%	UV curing; 10 mW/cm², 3 min	V_{Th} ↓ (from 18.2 to 6.8 V); response time reduced from 15.2 to 8.4 ms	H. Shim et al.[193]
E7	NOA65	SiO₂ (diameter 80 nm); 3 wt %	UV curing; 5 mW/cm², 60 min	operating voltage ↓ (from 29.6 to 27.1 V); V_{Th} ↓; CR ↓ (16%)	V. Sharma et al.[194]
SLC-1717 (40%)	BDDA/PEGDA600/HPMA/TMHA (2/3/12/8) (60%); Irgacure 651 photoinitiator was also used (0.5% of polymer)	TiO₂ (APTS and MPTS functionalized), 50 nm size was optimized due to its UV shielding characteristics; 1 wt %	UV curing; 5 mW/cm²; 10 min	off-state transmittance (T_{OFF}) ↓; on-state transmittance T_{ON} ↑; V_{Th} ↑; V_{Sat} ↑; contrast ratio ↑ (97.26); response time reduced to 13.4 ms; UV shielding characteristic was studied: 99.16% UV shielding without field, 95.9% with 60 V, 100 Hz signal	X. Wang et al.[195]
SLC-1717	polymer: CHMA, 2-EHA, TMPTA, PEGDA 600; Irgacure 651 photoinitiator (0.5 wt % of polymer)	CeO₂ (20–50 nm); 0.2, 0.4, 0.6, 0.8 wt %	UV curing, 10 min	V_{Th} ↓ from 26.6 to 16.8 V; CR ↑ from 89.5 to 137.6 (optimum results for 0.8 wt % NPs)	L. Jinqian et al.[196]
SCB (49.5%)	polyvinyl acetate (PVAc) (49.5%)	metal NPs: AgNPs (globular, 150 nm), CuNPs (globular, 150 nm), SiNPs (spherical, 30–50 nm); dielectric NPs: SiO₂ (spherical, 30–50 nm); composite NPs: TaSi₂/Si; Ag/Si. (1 wt %)	SIPS (chlorobenzene was used as solvent)	dielectric anisotropy Δε ↑; response time ↓	S. V. Kalashnikov et al.[170]
BL036 (60%)	NOA65 (40%)	SiNPs (10–15 nm) (<2 wt %)	PIPS (5 mW/cm²), 2 h	relative transmission ↑; V_{Th} and conductivity ↓	D. Jayoti et al.[197]
BL036 (60%)	NOA65 (40%)	citrate buffer-stabilized gold nanoparticles (AuNPs) (concentration 1.5 and 3 μL; 5.5 × 10¹⁰ NPs/μL)	PIPS (3 mW/cm²), 2 h	relative transmission ↑ 22%; CR ↑ 54%; V_{Th} ↓ 13%; E_g ↑; blue shift in PL spectra with increased intensity	A. Singh et al.[198]
E7 (50%)	NOA65 (50%)	azo and anthraquinone dye (0.0312, 0.0625, 0.1248, and 0.2494 wt %)	PIPS (2 mW/cm²), 1 h	CR ↑; T_{ON} for anthraquinone dyes ↑; V_{Th} ↓	P. Kumar et al.[199]
E7 (60%)	NOA65 (40%)	carbon NPs (size 100 nm; 0.0005%, 0.001%, 0.005%, 0.01%, 0.05%, 0.1%)	PIPS (8 mW/cm²), 1 h	CR ↑; V_{Th} ↓; relative transmission ↑	A. Katariya-Jain et al.[200]
E7	NOA65	orange azo dichroic dye (0.0625%, 0.125%, 0.25%, 0.5%, and 1%)	PIPS (2 mW/cm²), 1 h	T_{NI} ↓; CR ↑ (for lower dye concentrations), V_{Th} ↓	V. Sharma et al.[201]
E63 (25%)	NOA65 (75%)	Methyl Red azodye (1, 3, and 5 wt %)	TIPS (80 °C, 2 h)	V_{Th} ↓; K_{11} ↓; f_R ↑, relaxation time ↓	G. Önsal et al.[202]
TEB30 (35%)	acrylic monomer (EB8301), photoinitiator (RB and NPG), cross-linking agent (NVP), surfactant (S271) (45:0.15:0.4:10:10)	CuO nanorods (length 1–2 μm, diameter 40–60 nm)	PIPS	conductivity ↑, dielectric constant ↑ (40 times)	Z. Jiang et al.[203]
PCH5	acrylate-based monomer	functionalized single-walled carbon nanotubes (SWCNTs)	PIPS	response time ↓ (70%), V_{Th} ↓ (42%), relative transmission ↑	S. Shivaraja et al.[204]
SCB (25 wt %)	NOA81 (75 wt %)	InP/ZnS core/shell nanocrystals coated with oleylamine ligands (0.1 wt %)	PIPS	relative transmission ↑	S. Gandhi et al.[205]
SLC1717 (70 wt %)	n-lauryl acrylate (LA), 1,4-butanedioldiacrylate (BDDA) (mixture of prepolymers), benzoin methyl ether 651 (photoinitiator) (29 + 1 wt %)	surfactant-modified ZnS:Mn nanoparticles	PIPS (100 mW/cm², 15 min)	driving voltage ↓, response time ↓	L. Wang et al.[206]

[a]Here, ↑ and ↓ represent the increment and decrement of the corresponding parameter, respectively.
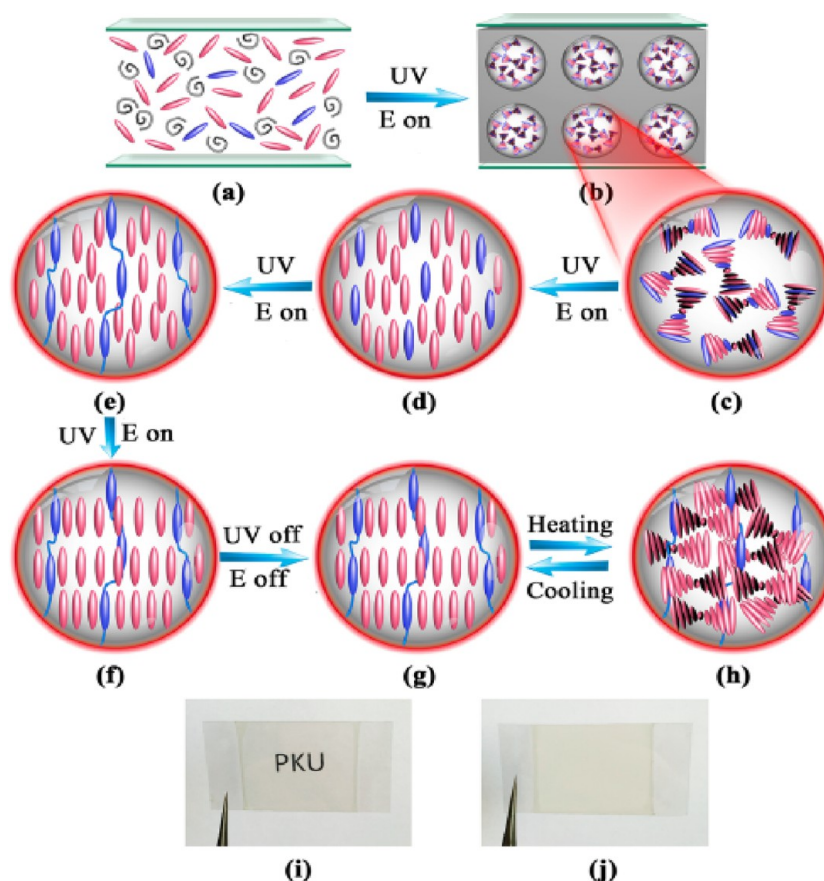
Figure 10. Pictorial representation of the film preparation. (a) Homogeneous isotropic mixture positioned between two plastic sheet pieces (b) The liquid crystalline mixture and polymer matrix undergo a microphase separation. (c) Random orientation of LC mixture within a particular droplet (d) Homeotropic alignment of LC mixture. (f) Slow conversion of N* phase into SmA phase upon utilization of monomers that are photopolymerizable. (g) Homeotropic alignment of the SmA phase within a LC droplet. (h) The focal-conic texture exhibiting the formation of N* phase within LC droplets due to induction by heat. (i, j) Photographs of the film (at temperature lower than the T_{NI}) in the transparent and opaque states, respectively. Reprinted with permission from ref 208. Copyright 2017 American Chemical Society.

ratio and find extensive applications in smart windows due to their greater haze and ability to achieve better privacy. However, dye contamination affects the performance of these devices. The encapsulation of dye in monodispersed capsules has been proposed to overcome these challenges and enhance the degree of commercialization of electric smart windows.[68] Furthermore, the exploitation of salt and photochromic dichroic dye-doped CLC in the fabrication of hybrid photo- and electrical-controllable smart window leads to better switching characteristics from OFF-state to ON-state, enabling the window to automatically dim when sunlight gets intense.[210]

Since the indium−tin oxide (ITO) layer, which serves as the transparent conducting electrode (TCE), accounts for more than half of the cost of the technology, existing LC-based smart windows have not yet gained momentum in the consumer market. In recent years, the implementation of low-cost hybrid TCEs based on different nanomaterials such as aluminum-doped zinc oxide, conducting polymer, graphene, carbon nanotubes, etc., has been proposed as a revolutionary alternative for ITO, with no loss of device performance in contrast to traditional ITO-based devices. These newly engineered electrodes offer the advantages of increased near-infrared heat shielding and superior light manage-ment.[54,211−219] However, the deployment of these materials is quite complicated, involving an expensive fabrication

procedure, and the materials possess low stability, less transparency, and nonuniform electric field distribution.[220] TiO$_2$/Ag(Cu)/TiO$_2$ (TCAT)-based PDLC devices exhibited 81.9%, 84.9%, 81.9%, and 79.9% ON-state transmittance for thicknesses of Ag(Cu) varying as 7, 9, 11, and 13 nm respectively. The device exhibited excellent heat shielding capability by providing a 4.6 °C lower temperature in the ON-state when compared with their ITO counterparts.[211] I. Mondal et al. proposed the deployment of a solution-processed SnO$_2$ film coated on a gold mesh electrode as a replacement for conventional ITO-based electrode in PDLC-based smart windows. Their group fabricated a large scale PDLC device (10 × 10 cm^2) with Al mesh electrodes spray-coated with SnO$_2$, exhibiting 13 and 161 ms response and recovery times, respectively, and high stability even after 400 days of storage.[221] Recently, Park and Kim[222] designed a highly stretchable PDLC system suitable for smart windows. Polyur-ethane (PU) substrates were coated with Ag NWs mixed with PEDOT:PSS to form highly transparent and stretchable hybrid electrodes superior to the conventional ITO/PU electrodes. The so-fabricated smart windows were found to exhibit 56% (at 80 V) and 2% (at 0 V) transmittance in the ON- and OFF-states, respectively, with stretching ability up to 30% without any damage. The results are illustrated in Figure 11, where Figure 11a and b compare the optical transmittance of the two systems (conventional ITO-based electrodes and the novel Ag
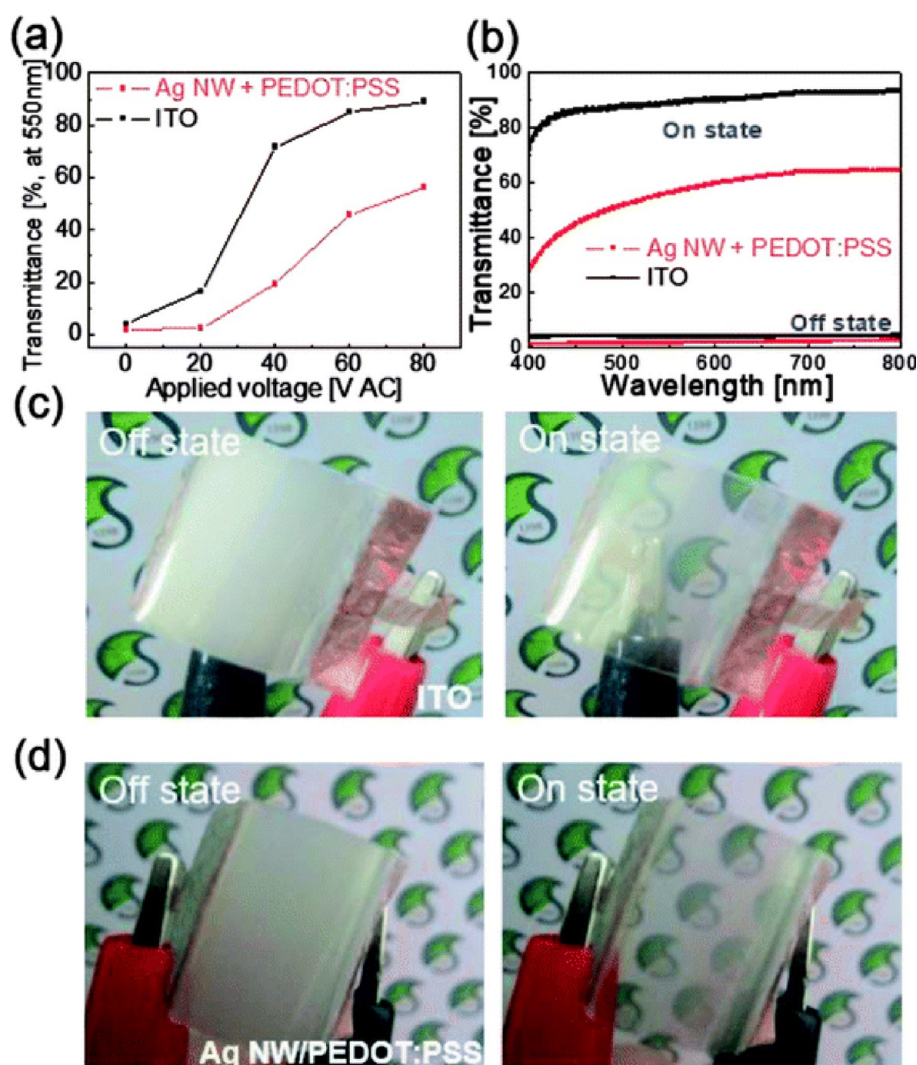
Figure 11. (a) Transmittance of PDLC-based smart window was a function of applied voltage. (b) On and off-state transmittance of a PDLC-based smart window for the two different type of electrode materials as a function of wavelength. Photographs of PDLC-based smart windows in the off and on-state (c) with ITO electrodes and (d) with Ag NW/PEDOT:PSS hybrid TSEs. Reproduced from ref 222. Available under a CC-BY 3.0 license. Copyright 2018 J. Park and H. Kim.

NW/PEDOT:PSS electrodes) with increasing AC voltages and increasing wavelength (from 400 to 800 nm), respectively. Corresponding images of the two PDLC systems in the ON- and OFF-states are depicted in Figure 11c and d, respectively. Despite demonstrating a greater ON-state transmittance than the PDLC-based smart window utilizing Ag NW/PEDOT:PSS hybrid transparent and stretchable electrode (TSE) materials, the brittleness of the ITO electrode precludes its application in stretchable PDLC-based smart windows.

Generally, small-scale windows were prepared by different researchers using capillary action for injecting PDLC samples in the windows. However, this method could not be used the large-scale production of windows/shutters with greater dimensions. For this purpose, lamination of PDLC onto a flexible plastic sheet (attached to a rigid glass plate) via a roll-to-roll process has been used; however, this method also possesses some disadvantages for long-term use of the material, as the atmospheric conditions affect the plastic used in the shutters adversely and start degrading it over a period of time. Along with this, the constant exposure to ultraviolet radiation leads to a yellowish appearance of the glazing that deteriorates

its physical appearance. To eliminate these limitations, Naila Nasir et al. developed a large (15×15 cm^2) switchable window using the vacuum glass coupling technique employing a wire-bar coater containing LC E7, polymer NOA65, and SiO$_2$ NPs (60%, 35%, and 5 wt %, respectively) and observed around 70% change in its transmittance of OFF- and ON-states when driven at 60 V and 60 Hz AC signal, as shown in Figure 12.[223]

MXenes have also attracted significant attention as novel potential candidates in the fabrication of transparent and flexible devices. S. Kumar and his group combined the highly transparent and conducting properties of Ti$_3$C$_2$T$_X$ MXene with the flexibility of polyethylene terephthalate (PET) film for the fabrication of a PDLC-based smart window with an extremely low threshold voltage (<10 V) and high contrast ratio.[224] Furthermore, to make the PDLC-based switchable glazing suitable for retrofit building integration, the use of an acrylic sheet was previously proposed, which resulted in a reduction of overall weight of the system by 21% with overall heat transfer coefficients below 1.1 W/m^2·K in ON- and OFF-states and the lowest solar heat gain coefficient of 0.23.[225]
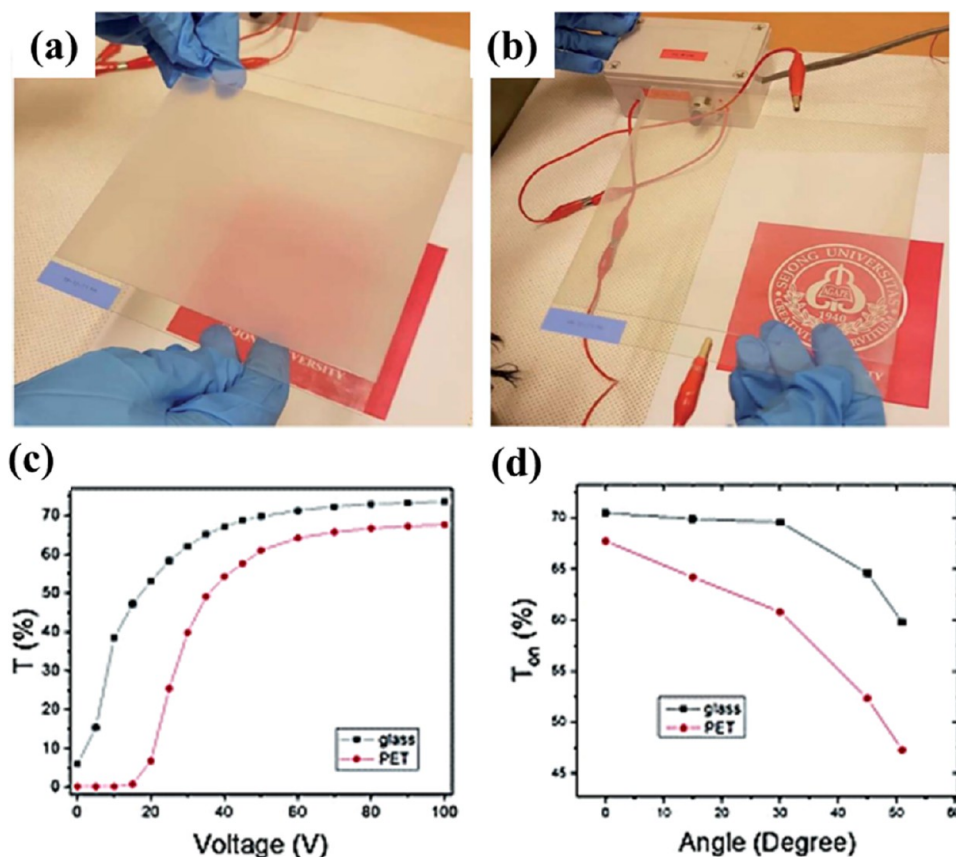
Figure 12. PDLC device developed using the vacuum-glass coupling technique: (a) opaque in off state and (b) transparent in on state. The corresponding change in the transmittance of the device as a function of (c) the applied voltage and (d) the angle of incidence of light. Reproduced with permission from ref 223. Available under a CC-BY 3.0 license. Copyright 2020 Y. Seo et al.

The real-time commercial applications of PDLCs in smart windows are limited because of their low UV-shielding characteristics. A breakthrough in this field occurred with the demonstration of novel PDLC composite films doped with TiO_2 NPs chemically functionalized by 3-aminopropyltriethoxysilane (APTS) and 3-methacryloxypropyltrimethoxysilane (MPTS), respectively. TiO_2(MPTS)/PDLC composite films were observed to shield UV light by 95.9% in the ON-state and by 99.16% in the OFF-state with enhanced response time and contrast ratio.[195] Smart windows with a radiative heat management capability have gained prominence. PDLC-based smart switchable glazing windows have become an alternative energy-saving solution for achieving visual comfort and reducing energy consumption.[129,226−232] Energy conservation in smart windows can also be achieved if the smart windows are coupled with switchable passive radiative cooling (PRC) technology, so that the transmission of sunlight through the window can be modulated electrically along with spontaneous heat emission to the outer space. The introduction of mid-infrared emitting reactive monomers (such as cyclohexyl methacrylate (CHMA), 2,2,3,4,4,4-hexafluorobutyl methacrylate (HFMA), and PEGDA 600) into the conventional PDLC matrix can help in yielding such properties.[233] It is worth contemplating a recent report published by Ube et al., where they developed LCPC-based smart windows showing a high photoresponsive property to incident visible light. They introduced the *cis−trans* photoisomerization property of azobenzene derivatives in the system, by virtue of which the device exhibited optical switching from the transparent to opaque state without any artificial operation or any external power supply.[234]

5.3. Microlens Arrays

Since their introduction, LC-based adaptive lenses have offered numerous features, including low weight, inexpensiveness, electrical-tunability of focal length, etc., as compared to the conventionally employed mechanical lenses. Different methods of LC lens fabrication have been proposed so far, such as spherical electrode,[235] polymer network,[236] hole-patterned electrode (HPE),[237] multiple ring electrodes,[238] etc. However, the solid lens and LC layers that make up spherical electrode LC lenses need large volumes. The strong anchoring of polymer networks necessitates high addressing voltages for polymer network LC lenses. An HPE lens also requires a high voltage for expanding the fringing electric field to the lens' center, since an active electrode and an LC layer encase a thick dielectric layer in an HPE LC lens to create a quadratic phase distribution. LC lenses with many ring electrodes feature intricate addressing methods and electrode topologies. A radial gradient pretilt angle (RGPA) distribution on the cell substrate surface can simplify the electrode construction of an LC lens and greatly lower its operating voltage. C.J. Hsu et al. utilized the features of PDLCs with these lensing systems by using a photopolymerization technique for the generation of polymer gravels on the substrates to create the RGPA distribution.[239] A photocurable prepolymer NOA65-dispersed NLC E7 was filled in a cell fabricated with vertically aligned substrates. To create the RGPA distribution, the authors used a radial variable
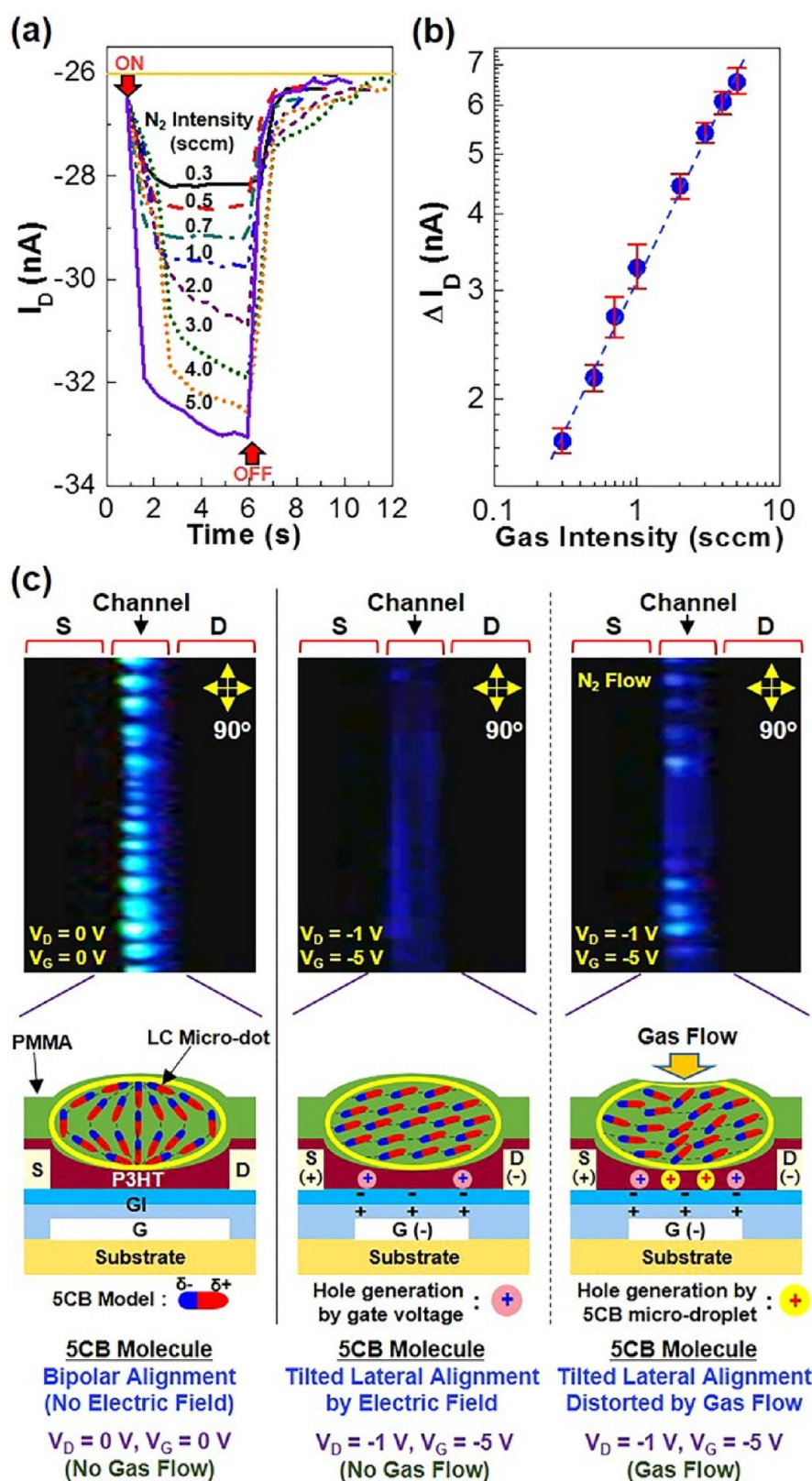
Figure 13. Sensing capabilities using weak gas flow stimulations and mechanism. (a) Variation of drain current (I_D) with time under stimulation with nitrogen gas flows (gas intensity of 0.3–5.0 sccm for 5 s) for the flexible PDLC-i-OFET devices. (b) Variation of drain current change (ΔI_D) with gas intensity before and after nitrogen gas stimulations. (c) Change of 5CB alignment in the channel region of PDLC-i-OFET devices as per variations in applied voltages and nitrogen gas stimulations: (top) polarized optical microscope images and (bottom) illustrations of the possible orientation of 5CB molecules in the LC microdots in the channel layers. Reproduced with permission from ref 253. Available under a CC-BY 4.0 license. Copyright 2017 Kim et al.

neutral density (RVND) filter during UV irradiation, which resulted in the preparation of self-assembled polymer gravels on the substrates. The proposed lens structure with aperture size of 5 mm displayed a low operating voltage (<4 V), good focusing quality, faster switch-off time (around 0.27 s using overdriving scheme), and smaller wavefront error (<0.08λ).

The phase modulation of an optically isotropic nano-PDLC has been utilized in the fabrication of polarization-dependent microlenticular lens arrays (MLAs).[240] The GRIN lens thus-formed, using interdigitated electrode systems, was found to exhibit 22 μm focal length with a very fast switching time (∼1 ms) between the transparent and lenticular lens state.

5.4. Display Technologies

PDLC technology has been found to be an efficient breakthrough for the development of active-matrix transparent display devices due to their good visibility, high transparency, polarizer-free operation, and low power consumption. On changing the driving voltage of the device, it can be controlled between the scattering state and the transparent state.[241] C. W. Su et al. utilized this PDLC technology for designing a 11.4 in. color active-matrix thin-film transistor (TFT) transparent LCD with 104 pixels per inch (PPI) and a resolution suitable for wide-screen video graphics array (WSVGA).[242] Monolithic integration of a CNT thin-film transistor driver circuit with PDLC pixels has been reported by S. Cong et al.,[243] who also demonstrated the employment of these CNT TFTs in the fabrication of active-matrix seven-segment PDLC displays.

Organic light emitting diodes (OLEDs) have recently seen the development of a revolutionary light-enhancing film based on PDLC systems. This film exhibits selective scattering in the directions of large incident angles, with LC droplets aligned unidirectionally along the normal direction of the film. Such films are found to demonstrate reduced total internal reflection (TIR) and hence their use in OLED systems may tend to increase the light efficiency of the display.[244] Furthermore, a switchable antipeeping film to facilitate the development of LCDs with a switchable viewing angle was prepared by L. Zhou et al., making the use of switching characteristics of PDLC films.[245] To prepare this film, nematic liquid crystalline material SLC-1717 was mixed in photocurable monomers Bis-EMA 15/PEGDA 600/HPMA/LMA in the ratio 50:4:6:24:16 along with 2.5 wt % Irgacure TPO photoinitiator, and the mixture was filled in a 7 μm thick cell via roll-to-roll process, followed by a photopolymerization process (365 nm, 5 mW/cm^2 intensity, 15 min duration). This film exhibited several excellent features over conventionally available antipeeping 3 M films, as it could be switched between a share mode and an antipeeping mode by the application of very small voltage (∼5 V) at a much faster speed and the viewing angle of the thus-developed LCD was found to be switchable between ±30° and ±60°. For the development of multicolored patterned displays, the fabrication of a dual-responsive electrochromic PDLC device has been proposed, which exhibited four switchable states corresponding to the application of different AC and DC fields. The light transmittance of the device was found to be altered with the AC field while the DC field aided in varying the color of the device.[246]

5.5. Sensors and Actuators

PDLCs have been proven to exhibit a great potential to be employed in modern cost-effective, easy-to-fabricate, and more versatile sensors and actuators. The inclusion of different dopants also tends to enhance the properties of these systems,

as discussed earlier. One such soft actuator film has been prepared by Z. Cheng et al.[247] by making use of the photothermal and photochemical properties of GO-doped PDLC systems owing to the phase transitions induced by its responsiveness to NIR-Vis-UV light. It was previously demonstrated that the PDLC structure formed by mixing a low-polarity LC, multiwalled carbon nanotubes (MWCNTs), and polydimethylsiloxane (PDMS) in an appropriate ratio leads to the construction of conductive paths in the active layer, which now behaves as a resistive pressure sensor exhibiting sensitivity up to 5.35 kPa^{-1}, faster response (<150 ms), great endurance, and showcases potential for use in wearable devices.[248] Many other such reports are available where functionalized CNTs and other nanoparticle-integrated PDLCs behave as sensing elements for different gaseous analytes such as acetone, ethanol, NO_2, dimethyl methylphosphonate (DMMP), etc. via measurement of alterations in the electrical resistance of the doped PDLC systems upon exposure to these analyte gases.[249−252]

M. Song et al.[253] demonstrated the possibility of simultaneous multisensing by combining the OFETs and the PDLC sensing layers through an innovative design of PDLC-integrated OFET-based flexible sensors ultrasensitive to different stimuli including weak N_2 gas flow (0.3 sccm), physical touch (0.6−4.8 g load), light, and heat (at a temperature of 25−70 °C). These wearable sensors have been designed on 200 μm-thick poly(ethylene naphthalate) (PEN) substrates with poly(methyl methacrylate) (PMMA)-dispersed 4,4′-pentylcyanobiphenyl (5CB) layers on the poly(3-hexylthiophene) (P3HT) channel layers of OFETs. Figure 13 presents the sensing performance of these devices upon exposure to very weak gas (N_2) flow. It has been illustrated that the net change in drain current (ΔI_D) was directly proportional to the nitrogen gas intensity, as a quick increment in the drain current of devices can be seen with the slightly increased intensity of N_2 exposure from 0.3 to 5 sccm (see Figure 13a and b); the simultaneous records of polarized optical micrographs are shown in Figure 13c. Several bright ellipsoid-like microspots were measured in the channel region in the field-off state, and a significantly darker channel area in the field-on state ($V_G = −5$ V and $V_D = −1$ V) converting again into a bright area upon exposure to N_2 gas is illustrated in Figure 13c. Song et al. observed the sensors to offer multisensing capabilities due to their responsive nature to two different stimulations at the same time. However, the selectivity for real multifunctionality requires further measurements in this field.

Several other researchers have also explored the potential applications of doped PDLC systems in sensors, displays, and polymer random fiber lasers. ZnCdSeS/ZnS-alloyed QD-doped PDLCs display such characteristics with a random laser threshold as low as 50 μJ/cm^2.[254] A magnetic NP-doped PDLC system exhibits exclusive features for a tunable microdevice whose locomotion can be controlled using a magnetic field of 30 mT.[255]

6. CONCLUSIONS AND FUTURE OUTLOOK

In summary, PDLCs represent a versatile class of materials with unique optical modulation capabilities derived from their composite structure of liquid crystal droplets dispersed within a polymer matrix. The ability to switch between transparent and opaque states makes PDLCs valuable for applications ranging from privacy windows and adaptive eyewear to

dynamic signage and electronic displays. The electro-optical switching mechanism of PDLCs enables rapid and reversible transitions between transparent and opaque states, making them ideal for applications requiring adjustable light modulation. The response time of PDLCs—the speed at which they switch between states—depends on factors such as liquid crystal viscosity, droplet size, and applied electric field strength. However, the electro-optical properties of PDLCs are strongly dependent on a number of factors such as the type and structure of the LC, the molecular structure of the polymerizable monomer, and polymerization conditions. These factors can seriously affect the microstructures of the polymer matrix, the size and shape of LC domains, and molecular interactions between the LC molecules and the polymer matrix. Advances in material design and fabrication techniques have led to PDLC variants with improved switching speed, lower operating voltages, and enhanced optical clarity. The selection of materials and fabrication techniques plays a pivotal role in optimizing the performance and functionality of PDLCs. Liquid crystal chemistry, polymer type, and processing methods influence droplet size distribution, mechanical strength, and electro-optical response dynamics. Common polymers used in PDLC matrices include acrylics, polyurethanes, and epoxies, chosen for their compatibility with liquid crystal phases and mechanical durability. Despite their promising characteristics, PDLCs face several challenges that hinder their widespread adoption and further development. Issues such as nonuniform droplet distribution, voltage-dependent switching behavior, and limited operational lifetimes under continuous stress necessitate ongoing research efforts. Improving droplet dispersion techniques, enhancing electro-optical response times, and exploring novel polymer chemistries are critical areas of focus for advancing PDLC technology. Future directions in PDLC research aim to overcome these challenges while exploring new applications and functionalities. Emerging trends include the integration of PDLCs with flexible substrates for wearable electronics, the development of environmentally sustainable materials, and the incorporation of advanced control algorithms for responsive light management systems. Collaborative efforts among academia, industry, and government sectors are crucial for accelerating innovation in PDLC technology and translating research discoveries into practical applications that address global challenges in energy efficiency, communication, and environmental sustainability. Continued research into optimizing fabrication techniques, enhancing electro-optical performance, and expanding application domains holds promise for unlocking the full potential of PDLCs in next-generation optical technologies.

ASSOCIATED CONTENT

Supporting Information

The Supporting Information is available free of charge at https://pubs.acs.org/doi/10.1021/acsmaterialsau.4c00122.

> Molecular structures of different LCs and polymers used in PDLC systems (PDF)

AUTHOR INFORMATION

Corresponding Authors

Rajiv Manohar − *Liquid Crystal Research Laboratory, Department of Physics, University of Lucknow, Lucknow, Uttar Pradesh 226007, India;* orcid.org/0000-0002-7441-8042; Email: rajiv.manohar@gmail.com

Kamal Kumar Pandey − *Soft Condensed Matter Lab, Department of Physics, Sri Jai Narain Misra PG College, Lucknow, Uttar Pradesh 226001, India;* orcid.org/0000-0002-4171-0784; Email: kamalpande27@gmail.com

Authors

Shikha Agarwal − *Liquid Crystal Research Laboratory, Department of Physics, University of Lucknow, Lucknow, Uttar Pradesh 226007, India;* orcid.org/0000-0002-7762-3308

Swastik Srivastava − *Liquid Crystal Research Laboratory, Department of Physics, University of Lucknow, Lucknow, Uttar Pradesh 226007, India*

Suraj Joshi − *Liquid Crystal Research Laboratory, Department of Physics, University of Lucknow, Lucknow, Uttar Pradesh 226007, India*

Shivangi Tripathi − *Liquid Crystal Research Laboratory, Department of Physics, University of Lucknow, Lucknow, Uttar Pradesh 226007, India*

Bhupendra Pratap Singh − *Department of Electro-Optical Engineering, National United University, Miao-Li 360, Taiwan;* orcid.org/0000-0002-0383-708X

Complete contact information is available at:
https://pubs.acs.org/10.1021/acsmaterialsau.4c00122

Author Contributions

S. Agarwal: writing—original draft preparation, conceptualization. **S. Srivastava**, **S. Joshi**, and **S. Tripathi**: formal analysis. **B.P. Singh**: writing—review and editing, methodology. **K.K. Pandey**: visualization and validation. **R. Manohar**: supervision, funding acquisition.

Notes

The authors declare no competing financial interest.

ACKNOWLEDGMENTS

LIST OF ABBREVIATIONS

LC	Liquid crystal/liquid crystalline material
2D/3D	Two dimensional/three dimensional
HD	High-definition
THz	Terahertz
PSLCs	Polymer-stabilized liquid crystals
PDLCs	Polymer-dispersed liquid crystals
LCPCs	Liquid crystal−polymer composites
PI	Polyimide
TN	Twisted-nematic (LC cells)
HA	Homogeneously aligned (LC cells)
PIPS	Polymerization-induced phase separation
TIPS	Temperature-induced phase separation
SIPS	Solvent-induced phase separation
EO	Electro-optical
LCD	Liquid crystal display
Bis-EMA 15	Bisphenol ethoxylate dimethacrylate
PEGDA	Polyethylene glycol diacrylate
TMPTA	Trimethylolpropane triacrylate
HPMA	Hydroxypropyl methacrylate
LMA	Lauryl methacrylate

TEGDA	Triethylene glycol diacrylate
TMPDE	Trimethylolpropane diallyl ether
TMPTMP	Trimethylolpropane tris(3-mercaptopropionate)
APTS	3-Aminopropyltriethoxysilane
MPTS	3-Methacryloxypropyltrimethoxysilane
4SH	Pentaerythritol tetrakis(2-mercaptoacetate)
GO	Graphene oxide
NLCMs	Nematic liquid crystal monomers
TMHA	3,5,5-Trimethylhexyl acrylate
LA	Lauryl acrylate (LA)
BDDA	Butane-1,4-diyl diacrylate
C6M	2-Methyl-1,4-phenylene bis(4-((6-(acryloyloxy)-hexyl)oxy)benzoate)
I651	Irgacure 651
HAPN	Homeotropically aligned polymer network
PU	Polyurethane
PEN	Poly(ethylene naphthalate)
PMMA	Poly(methyl methacrylate)
P3HT	Poly(3-hexylthiophene)
POSS	Polyhedral oligomeric silsesquioxane
CHMA	Cyclohexyl methacrylate
HFMA	2,2,3,4,4,4-Hexafluorobutyl methacrylate
WSVGA	Wide-screen video graphics array
TFT	Thin-film transistor
TSE	Transparent and stretchable electrode
PPI	Pixel per inch
RGPA	Radial gradient pretilt angle
RVND	Radial variable neutral density
MLA	Microlenticular lens array
MWCNTs	Multiwalled carbon nanotubes
PDMS	Polydimethylsiloxane

■ REFERENCES

(1) Lin, Y.-H.; Wang, Y.-J.; Reshetnyak, V. Liquid crystal lenses with tunable focal length. *Liquid Crystals Reviews* **2017**, *5* (2), 111–143.

(2) Kim, T. H.; Kim, M.; Manda, R.; Lim, Y. J.; Cho, K. J.; Hee, H.; Kang, J.-W.; Lee, G.-D.; Lee, S. H. Flexible Liquid Crystal Displays Using Liquid Crystal-polymer Composite Film and Colorless Polyimide Substrate. *Curr. Opt. Photon.* **2019**, *3* (1), 66–71.

(3) Choi, H.-M.; Choi, J.-G.; Kim, E.-S. Dual-View Three-Dimensional Display Based on Direct-Projection Integral Imaging with Convex Mirror Arrays. *Applied Sciences* **2019**, *9* (8), 1577.

(4) Moser, S.; Ritsch-Marte, M.; Thalhammer, G. Model-based compensation of pixel crosstalk in liquid crystal spatial light modulators. *Opt. Express* **2019**, *27* (18), 25046–25063.

(5) Schadt, M. D. Nematic liquid crystals and twisted-nematic LCDs. *Liq. Cryst.* **2015**, *42*, 646–652.

(6) Hsu, C. W.; Zhen, B.; Qiu, W.; Shapira, O.; DeLacy, B. G.; Joannopoulos, J. D.; Soljačić, M. Transparent displays enabled by resonant nanoparticle scattering. *Nat. Commun.* **2014**, *5* (1), 3152.

(7) Zhu, R.; Xu, S.; Hong, Q.; Wu, S.-T.; Lee, C.; Yang, C.-M.; Lo, C.-C.; Lien, A. Polymeric-lens-embedded 2D/3D switchable display with dramatically reduced crosstalk. *Appl. Opt.* **2014**, *53* (7), 1388–1395.

(8) Meng, Y.; Lyu, Y.; Chen, L. L.; Yu, Z.; Liao, H. Motion parallax and lossless resolution autostereoscopic 3D display based on a binocular viewpoint tracking liquid crystal dynamic grating adaptive screen. *Opt. Express* **2021**, *29* (22), 35456–35473.

(9) Guoqiang, L. Adaptive lens. In *Progress in optics*, Vol. 55; Elsevier, 2010; pp 199–283.

(10) Shcherbinin, D.; Konshina, E. Impact of titanium dioxide nanoparticles on purification and contamination of nematic liquid crystals. *Beilstein J. Nanotechnol.* **2017**, *8*, 2766–2770.

(11) Hsu, C. J.; Singh, B. P.; Antony, M.; Selvaraj, P.; Manohar, R.; Huang, C. Y. Liquid crystal lens with doping of rutile titanium dioxide nanoparticles. *Opt. Express* **2020**, *28* (15), 22856–22866.

(12) Hsu, C. J.; Singh, B. P.; Selvaraj, P.; Antony, M.; Manohar, R.; Huang, C. Y. Superior improvement in dynamic response of liquid crystal lens using organic and inorganic nanocomposite. *Sci. Rep.* **2021**, *11* (1), No. 17349.

(13) Algorri, J.; Morawiak, P.; Bennis, N.; Zografopoulos, D.; Urruchi, V.; Rodríguez-Cobo, L.; Jaroszewicz, L. R.; Sánchez-Pena, J.; López-Higuera, J. M. Positive-negative tunable liquid crystal lenses based on a microstructured transmission line. *Sci. Rep.* **2020**, *10*, 10153.

(14) Chen, H.-S.; Wang, Y.-J.; Chen, P.-J.; Lin, Y.-H. Electrically adjustable location of a projected image in augmented reality via a liquid-crystal lens. *Opt. Express* **2015**, *23* (22), 28154–28162.

(15) Huang, Y.; Liao, E.; Chen, R.; Wu, S.-T. Liquid-Crystal-on-Silicon for Augmented Reality Displays. *Applied Sciences* **2018**, *8* (12), 2366.

(16) Isić, G.; Vasić, B.; Zografopoulos, D.; Beccherelli, R.; Gajić, R. Electrically Tunable Critically Coupled Terahertz Metamaterial Absorber Based on Nematic Liquid Crystals. *Phys. Rev. Appl.* **2015**, *3*, 064007 DOI: 10.1103/PhysRevApplied.3.064007.

(17) Schadt, M.; Schmitt, K.; Kozinkov, V.; Chigrinov, V. Surface-induced parallel alignment of liquid crystals by linearly polymerized photopolymers. *Jpn. J. Appl. Phys.* **1992**, *31* (7R), 2155.

(18) Kondo, M.; Yu, Y.; Ikeda, T. How does the initial alignment of mesogens affect the photoinduced bending behavior of liquid-crystalline elastomers? *Angew. Chem., Int. Ed.* **2006**, *45* (9), 1378–1382.

(19) Ishihara, S.; Mizusaki, M. Alignment control technology of liquid crystal molecules. *J. Soc. Inf. Dispersion* **2020**, *28* (1), 44–74.

(20) Podoliak, N.; Buchnev, O.; Herrington, M.; Mavrona, E.; Kaczmarek, M.; Kanaras, A. G.; Stratakis, E.; Blach, J.-F.; Henninot, J.-F.; Warenghem, M. Elastic constants, viscosity and response time in nematic liquid crystals doped with ferroelectric nanoparticles. *Rsc Advances* **2014**, *4* (86), 46068–46074.

(21) Vardanyan, K. K.; Sita, D. M.; Walton, R. D.; Saidel, W. M.; Jones, K. M. Cyanobiphenyl liquid crystal composites with gold nanoparticles. *RSC Adv.* **2013**, *3* (1), 259–273.

(22) Kaczmarek, M.; Buchnev, O.; Nandhakumar, I. Ferroelectric nanoparticles in low refractive index liquid crystals for strong electro-optic response. *Appl. Phys. Lett.* **2008**, *92*, 103307.

(23) Acharya, S.; Kundu, S.; Hill, J. P.; Richards, G. J.; Ariga, K. Nanorod-Driven Orientational Control of Liquid Crystal for Polarization-Tailored Electro-Optic Devices. *Adv. Mater.* **2009**, *21* (9), 989–993.

(24) Basu, R.; Iannacchione, G. S. Evidence for directed self-assembly of quantum dots in a nematic liquid crystal. *Phys. Rev. E* **2009**, *80* (1), No. 010701.

(25) Singh, B. P.; Sikarwar, S.; Pandey, K. K.; Duraisamy, S.; Gupta, S. K.; Manohar, R. Nematic Liquid Crystals Dispersed with Thermoelectric Gallium Oxide (Ga2O3) Microrods: A Perspective for Improving the Response Time of Electro-Optical Devices. *J. Phys. Chem. C* **2022**, *126* (37), 15924–15935.

(26) Davidson, Z. S.; Huang, Y.; Gross, A.; Martinez, A.; Still, T.; Zhou, C.; Collings, P. J.; Kamien, R. D.; Yodh, A. Deposition and drying dynamics of liquid crystal droplets. *Nat. Commun.* **2017**, *8*, 15642.

(27) Tongcher, O.; Sigel, R.; Landfester, K. Liquid crystal nanoparticles prepared as miniemulsions. *Langmuir* **2006**, *22* (10), 4504–4511.

(28) Bouteiller, L.; Barny, P. L. Polymer-dispersed liquid crystals: preparation, operation and application. *Liq. Cryst.* **1996**, *21* (2), 157–174.

(29) Higgins, D. A. Probing the mesoscopic chemical and physical properties of polymer-dispersed liquid crystals. *Adv. Mater.* **2000**, *12* (4), 251–264.

(30) Wang, P.-C.; MacDiarmid, A. G. Integration of polymer-dispersed liquid crystal composites with conducting polymer thin films toward the fabrication of flexible display devices. *Displays* **2007**, *28* (3), 101–104.

(31) Vicari, L. *Optical applications of liquid crystals*; CRC Press: Boca Raton, FL, 2003.

(32) Wu, S. T.; Yang, D. K. *Fundamentals of Liquid Crystal Devices*; Wiley, 2006.

(33) Li, C.-Y.; Wang, X.; Liang, X.; Sun, J.; Li, C.-X.; Zhang, S.-F.; Zhang, L.-Y.; Zhang, H.-Q.; Yang, H. Electro-Optical Properties of a Polymer Dispersed and Stabilized Cholesteric Liquid Crystals System Constructed by a Stepwise UV-Initiated Radical/Cationic Polymerization. *Crystals* 2019, 9 (6), 282.

(34) Rajaram, C. V.; Hudson, S. D.; Chien, L. C. Effect of Polymerization Temperature on the Morphology and Electrooptic Properties of Polymer-Stabilized Liquid Crystals. *Chem. Mater.* 1996, 8 (10), 2451−2460.

(35) Li, C.; Chen, M.; Zhang, L.; Shen, W.; Liang, X.; Wang, X.; Yang, H. An electrically light-transmittance-switchable film with a low driving voltage based on liquid crystal/polymer composites. *Liq. Cryst.* 2020, 47 (1), 106−113.

(36) Kim, H. N.; Yang, S. Responsive smart windows from nanoparticle−polymer composites. *Adv. Funct. Mater.* 2020, 30 (2), No. 1902597.

(37) Xia, Y.; Liang, X.; Jiang, Y.; Wang, S.; Qi, Y.; Liu, Y.; Yu, L.; Yang, H.; Zhao, X. Z. High-efficiency and reliable smart photovoltaic windows enabled by multiresponsive liquid crystal composite films and semi-transparent perovskite solar cells. *Adv. Energy Mater.* 2019, 9 (33), No. 1900720.

(38) Ramanitra, H.; Chanclou, P.; Vinouze, B.; Dupont, L. Application of polymer dispersed liquid crystal (PDLC) nematic: optical-fiber variable attenuator. *Mol. Cryst. Liq. Cryst.* 2003, 404 (1), 57−73.

(39) Yu, P.; Su, Y.; He, N.; Yang, H.; Song, W.; He, Z.; Miao, Z. A flexible reverse-mode liquid crystal/polymer composite film with low driving voltage and high stability for energy-efficient smart windows. *Liq. Cryst.* 2024, 51, 1757.

(40) Zhao, Y.; Yi, H.; He, Z.; Gao, H.; Gao, J.; Wang, D.; Luan, Y. Effect of SiO2-doped nanoparticle/electrostatic spinning system on the electro-optical properties of polymer dispersed liquid crystals for smart windows. *Liq. Cryst.* 2024, 51, 1768.

(41) Yin, W.; Zhao, Y.; Jiao, X.; Gao, H.; Zhao, Y.; Wang, D.; Luan, Y.; Miao, Z. Intelligent switchable nanomaterials doped optical switches with PDLC-PVA-PSCLC bilayer liquid crystal structure for smart windows. *Liq. Cryst.* 2024, 51, 1149.

(42) Chauhan, G.; Malik, P.; Malik, P.; Deep, A. Improved performance of cadmium selenide quantum dots-doped polymer stabilized cholesteric liquid crystals for light shutter. *Liq. Cryst.* 2023, 50 (15), 2540−2551.

(43) Chauhan, G.; Malik, P.; Kaur, G.; Singh, A. K.; Deep, A.; Malik, P. Surface induced effects on the dielectric and optical properties of polymer-stabilized cholesteric liquid crystal composites. *Ferroelectrics* 2024, 618 (2), 421−431.

(44) Ditter, D.; Chen, W.-L.; Best, A.; Zappe, H.; Koynov, K.; Ober, C. K.; Zentel, R. J. j. o. M. C. C. MEMS analogous micro-patterning of thermotropic nematic liquid crystalline elastomer films using a fluorinated photoresist and a hard mask process. *Journal of Materials Chemistry C* 2017, 5 (47), 12635−12644.

(45) Waits, C.; Morgan, B.; Kastantin, M.; Ghodssi, R. J. S. Physical, A. A. Microfabrication of 3D silicon MEMS structures using gray-scale lithography and deep reactive ion etching. *Sensors and Actuators A: Physical* 2005, 119 (1), 245−253.

(46) Wen, Z.; McBride, M. K.; Zhang, X.; Han, X.; Martinez, A. M.; Shao, R.; Zhu, C.; Visvanathan, R.; Clark, N. A.; Wang, Y.; et al. J. M. Reconfigurable LC elastomers: using a thermally programmable monodomain to access two-way free-standing multiple shape memory polymers. *Macromolecules* 2018, 51 (15), 5812−5819.

(47) Wang, Y.; Liu, J.; Yang, S. J. A. P. R. Multi-functional liquid crystal elastomer composites. *Appl. Phys. Rev.* 2022, 9, 011301.

(48) Rastogi, P.; Njuguna, J.; Kandasubramanian, B. J. E. P. J. Exploration of elastomeric and polymeric liquid crystals with photothermal actuation: a review. *Eur. Polym. J.* 2019, 121, No. 109287.

(49) Jiang, H.; Li, C.; Huang, X. J. N. Actuators based on liquid crystalline elastomer materials. *Nanoscale* 2013, 5 (12), 5225−5240.

(50) Sun, J.; Wu, S.-T. Recent advances in polymer network liquid crystal spatial light modulators. *J. Polym. Sci. B* 2014, 52, 183.

(51) Takizawa, K.; Fujii, T.; Kawakita, M.; Kikuchi, H.; Fujikake, H.; Yokozawa, M.; Murata, A.; Kishi, K. Spatial light modulators for projection displays. *Appl. Opt.* 1997, 36 (23), 5732−5747.

(52) Marinov, Y. G.; Hadjichristov, G. B.; Petrov, A. G. Single-layered PDLC films for electrically variable laser light reflection application. *Optics and Lasers in Engineering* 2010, 48 (12), 1161−1165.

(53) Lu, Y.; Wang, X.; Yang, D.; Zhong, Z.; Gao, H.; Du, X.; Zhao, Y.; He, Z.; Cao, H.; Yang, Z.; et al. PDLC flexible films with multiple fluorescence and voltage modulated modes and intelligent coding for applications in anti-counterfeiting and transparent displays. *Chemical Engineering Journal* 2024, 496, No. 153742.

(54) Kumar, S.; Park, H. M.; Nguyen, V. H.; Kim, M.; Nasir, N.; Kumar, M.; Seo, Y. Application dependent stability of Ti3C2Tx MXene in PDLC-based smart-windows. *Ceram. Int.* 2022, 48 (23), 35092−35099.

(55) Baratta, M.; Nezhdanov, A.; Mashin, A. I.; Curcio, M.; Cirillo, G.; Nicoletta, F. P.; De Filpo, G. J. L. C. Electrochromic reverse-mode PDLCs as smart windows. *Liq. Cryst.* 2023, 50 (13−14), 2295−2305.

(56) Ghosh, A.; Mallick, T. J. R. E. Evaluation of colour properties due to switching behaviour of a PDLC glazing for adaptive building integration. *Renewable Energy* 2018, 120, 126−133.

(57) Hadjichristov, G. B.; Marinov, Y. G.; Petrov, A. G. Electrically and spatially controllable PDLC phase gratings for diffraction and modulation of laser beams. *AIP Conf. Proc.* 2016, 1722, 290007.

(58) Fernández, R.; Gallego, S.; Márquez, A.; Francés, J.; Martínez, F. J.; Pascual, I.; Beléndez, A. Analysis of holographic polymer-dispersed liquid crystals (HPDLCs) for tunable low frequency diffractive optical elements recording. *Opt. Mater.* 2018, 76, 295−301.

(59) Trushkevych, O.; Reshetnyak, V.; Turvey, M.; Edwards, R. S. Polymer-dispersed liquid-crystal coatings for ultrasound visualization: Experiment and theory. *Phys. Rev. E* 2024, 109 (6), No. 064701.

(60) Karapinar, R; O'Neill, M; Hird, M Polymer dispersed ferroelectric liquid crystal films with high electro-optic quality. *J. Phys. D: Appl. Phys.* 2002, 35 (9), 900.

(61) Katariya- Jain, A.; Mhatre, M.; Dierking, I.; Deshmukh, R. Enhanced Thermo-Electro-Optical and Dielectric Properties of Carbon Nanoparticle-Doped Polymer Dispersed Liquid Crystal Based Switchable Windows. *J. Mol. Liq.* 2024, 393, No. 123575.

(62) Lu, Y.; Wei, J.; Shi, Y.; Jin, O.; Guo, J. Effects of fabrication condition on the network morphology and electro-optical characteristics of polymer-dispersed bistable smectic A liquid crystal device. *Liq. Cryst.* 2013, 40 (5), 581−588.

(63) Yaroshchuk, O.; Elouali, F.; Maschke, U. Control of phase separation and morphology of thiol−ene based PDLCs by curing light intensity. *Opt. Mater.* 2010, 32 (9), 982−989.

(64) Jo, Y.-S.; Choi, T.-H.; Ji, S.-M.; Yoon, T.-H. Control of haze value by dynamic scattering in a liquid crystal mixture without ion dopants. *AIP Adv.* 2018, 8 (8), 085004 DOI: 10.1063/1.5030764.

(65) Saeed, M. H.; Zhang, S.; Cao, Y.; Zhou, L.; Hu, J.; Muhammad, I.; Xiao, J.; Zhang, L.; Yang, H. Recent Advances in The Polymer Dispersed Liquid Crystal Composite and Its Applications. *Molecules* 2020, 25 (23), 5510.

(66) Oh, S.-W.; Baek, J.-M.; Heo, J.; Yoon, T.-H. Dye-doped cholesteric liquid crystal light shutter with a polymer-dispersed liquid crystal film. *Dyes Pigm.* 2016, 134, 36−40.

(67) Huang, C.-Y.; Lin, S.-H. Organic Solvent Sensors Using Polymer-Dispersed Liquid Crystal Films with a Pillar Pattern. *Polymers* 2021, 13 (17), 2906.

(68) Kim, M.; Park, K. J.; Seok, S.; Ok, J. M.; Jung, H.-T.; Choe, J.; Kim, D. H. Fabrication of Microcapsules for Dye-Doped Polymer-Dispersed Liquid Crystal-Based Smart Windows. *ACS Appl. Mater. Interfaces* 2015, 7 (32), 17904−17909.

(69) Murray, J.; Ma, D.; Munday, J. N. Electrically Controllable Light Trapping for Self-Powered Switchable Solar Windows. *ACS Photonics* **2017**, *4* (1), 1−7.

(70) Kamal, W.; Li, M.; Lin, J.-D.; Parry, E.; Jin, Y.; Elston, S. J.; Castrejón-Pita, A. A.; Morris, S. M. Spatially Patterned Polymer Dispersed Liquid Crystals for Image-Integrated Smart Windows. *Advanced Optical Materials* **2022**, *10* (3), No. 2101748.

(71) Katariya-Jain, A.; Deshmukh, R. R. Effects of dye doping on electro-optical, thermo-electro-optical and dielectric properties of polymer dispersed liquid crystal films. *J. Phys. Chem. Solids* **2022**, *160*, No. 110363.

(72) Wang, X.; Hu, W.; Chen, H.; Saeed, M. H.; Huang, J.; Hu, J.; Ren, Y.; Xu, J.; Zhang, L.; Yu, M.; et al. Effects of chemically functionalized TiO2 nanoparticles on the UV-shielding characteristics of polymer-dispersed liquid crystals. *Polymers Advanced Technologies* **2022**, *33* (5), 1561−1568.

(73) Wu, Y.; Zhao, Y.; Li, X.; Gao, H.; Guo, Z.; Wang, D.; Luan, Y.; Wang, L. Preparation and Characterization of Bilayer Polymer-Dispersed Liquid Crystals Doped with Gd2O3 Nanoparticles and Rhodamine B Base Fluorescent Dye. *Molecules* **2024**, *29* (5), 1126.

(74) Singh, S.; Srivastava, J.; Singh, R. Polymer Dispersed Liquid Crystals. In *Liquid Crystalline Polymers*, Vol. 1; Springer Nature, 2016; pp 195−250.

(75) Montgomery, G. P.; Smith, G. W.; Vaz, N. A. Polymer-Dispersed Liquid Crystal Films. In *Liquid Crystalline and Mesomorphic Polymers*; Shibaev, V. P., Lam, L., Eds.; Springer: New York, NY, 1994; pp 149−192.

(76) Fergason, J. Polymer encapsulated liquid crystals for display and light control applications. *Tech. Digest SID Int. Symp.* **1985**, *16*, 68−70.

(77) Coates, D. Polymer-dispersed liquid crystals. *J. Mater. Chem.* **1995**, *5* (12), 2063−2072.

(78) Coates, D. Normal and reverse mode polymer dispersed liquid crystal devices. *Displays* **1993**, *14* (2), 94−103.

(79) Gotoh, T.; Murai, H. Preparation and characteristics of new reverse mode film of polymer dispersed liquid crystal type. *Appl. Phys. Lett.* **1992**, *60* (3), 392−394.

(80) De Filpo, G.; Formoso, P.; Mashin, A. I.; Nezhdanov, A.; Mochalov, L.; Nicoletta, F. P. A new reverse mode light shutter from silica-dispersed liquid crystals. *Liq. Cryst.* **2018**, *45*, 721−727.

(81) Cho, Y. H.; Kawakami, Y. A novel process for holographic polymer dispersed liquid crystal system via simultaneous photopolymerization and siloxane network formation. *Silicon Chemistry* **2007**, *3* (5), 219−227.

(82) Anuja, K.-J.; Deshmukh, R. R. An overview of HPDLC films and their applications. *Liq. Cryst.* **2022**, *49*, 589−604.

(83) Wang, K.; Zheng, J.; Gao, H.; Lu, F.; Sun, L.; Yin, S.; Zhuang, S. Tri-color composite volume H-PDLC grating and its application to 3D color autostereoscopic display. *Opt. Express* **2015**, *23*, 31436.

(84) Pavani, K.; Naydenova, I.; Raghavendra, J.; Martin, S.; Toal, V. Electro-optical switching of the holographic polymer-dispersed liquid crystal diffraction gratings. *Journal of Optics A: Pure and Applied Optics* **2009**, *11* (2), No. 024023.

(85) Liu, L.; Xuan, l.; Ma, J. Optical Performance of Organic Distributed Feedback Lasers Based on Holographic Polymer Dispersed Liquid Crystals. In *Photochemical Behavior of Multicomponent Polymeric-based Materials*; Rosu, D., P. M, V., Eds.; Advanced Structured Materials, Vol. *26*; Springer Nature, 2016; pp 379−405.

(86) Hulst, H. C.; van de Hulst, H. C. *Light Scattering by Small Particles*; Dover Publications, 1981.

(87) Zumer, S.; Doane, J. W. Light scattering from a small nematic droplet. *Phys. Rev. A Gen Phys.* **1986**, *34* (4), 3373−3386.

(88) Montgomery, G. P. Angle-dependent scattering of polarized light by polymer-dispersed liquid-crystal films. *Journal of the Optical Society of America B* **1988**, *5* (4), 774−784.

(89) Zumer, S. Light scattering from nematic droplets: Anomalous-diffraction approach. *Phys. Rev. A Gen Phys.* **1988**, *37* (10), 4006−4015.

(90) Kelly, J.; Wu, W.; Palffy-muhoray, P. Wavelength Dependence of Scattering in PDLC Films: Droplet Size Effects. *Molecular Crystals and Liquid Crystals Science and Technology. Section A. Molecular Crystals and Liquid Crystals* **1992**, *223* (1), 251−261.

(91) Kelly, J. R.; Wu, W. Multiple scattering effects in polymer dispersed liquid crystals. *Liq. Cryst.* **1993**, *14* (6), 1683−1694.

(92) Yang, D.-K.; Wu, S.-T. Liquid Crystal/Polymer Composites. In *Fundamentals of Liquid Crystal Devices*, 1st ed.; Wiley, 2006; pp 307−346.

(93) Kitzerow, H.-S. Polymer-dispersed liquid crystals From the nematic curvilinear aligned phase to ferroelectric films. *Liq. Cryst.* **1994**, *16* (1), 1−31.

(94) McCormick, D. T.; Chavers, R.; Guymon, C. A. J. M. Investigation of polymer nanostructure evolution during the formation of polymer/smectic liquid crystal composites. *Macromolecules* **2001**, *34* (20), 6929−6935.

(95) Klosowicz, S.; Piecek, W.; Dabrowski, R.; Perkowski, P. Switching of orthoconic antiferroelectric mixtures in PDLC system. *Mol. Cryst. Liq. Cryst.* **2004**, *422* (1), 21−26.

(96) Yamaguchi, M.; Matsukizono, H.; Okumura, Y.; Kikuchi, H. Nanostructured Polymer-Dispersed Liquid Crystals Using a Ferro-electric Smectic A Liquid Crystal. *Molecules* **2024**, *29* (20), 4837.

(97) Doane, J. W.; Golemme, A.; West, J. L.; Whitehead, J. B., Jr; Wu, B. G. Polymer Dispersed Liquid Crystals for Display Application. *Molecular Crystals and Liquid Crystals Incorporating Nonlinear Optics* **1988**, *165* (1), 511−532.

(98) Ondris-Crawford, R.; Boyko, E. P.; Wagner, B. G.; Erdmann, J. H.; Žumer, S.; Doane, J. W. Microscope textures of nematic droplets in polymer dispersed liquid crystals. *J. Appl. Phys.* **1991**, *69*, 6380−6386.

(99) Prishchepa, O. O.; Shabanov, A. V. e.; Zyryanov, V. Y.; Parshin, A.; Nazarov, V. G. J. J. l. Friedericksz threshold field in bipolar nematic droplets with strong surface anchoring. *Journal of experimental and Theoretical Physics Letters* **2007**, *84*, 607−612.

(100) Drzaic, P. S. J. M. C.; Crystals, L. A New Director Alignment for Droplets of Nematic Liquid Crystal with Low Bend-to-Splay Ratio. *Mol. Cryst. Liq. Cryst.* **1988**, *154*, 289−306.

(101) Springer, G. H.; Higgins, D. A. Toroidal Droplet Formation in Polymer-Dispersed Liquid Crystal Films. *J. Am. Chem. Soc.* **2000**, *122* (28), 6801−6802.

(102) Chiccoli, C.; Pasini, P.; Semeria, F.; Zannoni, C. Computer Simulations of Nematic Droplets with Toroidal Boundary Conditions. *Molecular Crystals and Liquid Crystals Science and Technology. Section A. Molecular Crystals and Liquid Crystals* **1992**, *221* (1), 19−28.

(103) Erdmann, J. H.; Žumer, S.; Doane, J. W. Configuration transition in a nematic liquid crystal confined to a small spherical cavity. *Phys. Rev. Lett.* **1990**, *64* (16), 1907−1910.

(104) Yan, B.; He, J.; Du, X.; Zhang, K.; Wang, S.; Pan, C.; Wang, Y. J. L. C. Control of liquid crystal droplet configuration in polymer dispersed liquid crystal with macro-iniferter polystyrene. *Liq. Cryst.* **2009**, *36* (9), 933−938.

(105) Zhou, F.; Ou-Yang, Z.; Xu, S.; Gao, H.; Zhang, B.; You, S. Configuration Transitions of Nematic Droplets in PDLC. *Mol. Cryst. Liq. Cryst.* **1997**, *304*, 47−58.

(106) Bodnar, V.; Lavrentovich, O.; Pergamenshchik, V. M. The threshold for the hedgehog-ring structural transition in nematic drops in an alternating electric-field. *Zh. Eksp. Teor. Fiz.* **1992**, *101* (1), 111−125.

(107) Kralj, S.; Žumer, S. Fr\`eedericksz transitions in supra-\ensuremath{\mu}m nematic droplets. *Phys. Rev. A* **1992**, *45* (4), 2461−2470.

(108) Malik, P.; Raina, K. K. Droplet orientation and optical properties of polymer dispersed liquid crystal composite films. *Opt. Mater.* **2004**, *27* (3), 613−617.

(109) Prishchepa, O.; Zyryanov, V.; Gardymova, A.; Shabanov, V. Optical Textures and Orientational Structures of Nematic and Cholesteric Droplets with Heterogeneous Boundary Conditions. *Mol. Cryst. Liq. Cryst.* **2008**, *489*, 84−93.

(110) Krakhalev, M. N.; Gardymova, A. P.; Prishchepa, O. O.; Rudyak, V. Y.; Emelyanenko, A. V.; Liu, J.-H.; Zyryanov, V. Y. Bipolar configuration with twisted loop defect in chiral nematic droplets under homeotropic surface anchoring. *Sci. Rep.* **2017**, *7* (1), No. 14582.

(111) Lin, Y.-H.; Ren, H.; Wu, Y.-H.; Liang, X.; Wu, S.-T. Surface anchoring effect on the morphology and performance of polymer-dispersed liquid crystal. In *Emerging Liquid Crystal Technologies*; SPIE, 2005; Vol. *5741*, pp 74−82.

(112) Carter, S. A.; LeGrange, J. D.; White, W.; Boo, J.; Wiltzius, P. Dependence of the morphology of polymer dispersed liquid crystals on the UV polymerization process. *J. Appl. Phys.* **1997**, *81* (9), 5992−5999.

(113) Kihara, H.; Kishi, R.; Miura, T.; Horiuchi, S.; Okada, Y.; Yase, K.; Ichijo, H. Thermomechanical analysis of a polymer dispersed liquid crystal containing a thermoplastic elastomer. *Liquid Crystals - LIQ CRYST* **2001**, *28*, 1655−1658.

(114) Hakemi, H.; Khenkin, M.; Tamari, R.; Gal-Fuss, D. Transient Phenomenon in Polymer-Dispersed Liquid Crystals. *Recent Prog. Mater.* **2020**, *2* (1), 006.

(115) Chen, L. G.; Shanks, R. Thermoplastic polymer-dispersed liquid crystals prepared from solvent-induced phase separation with predictions using solubility parameters. *Liq. Cryst.* **2007**, *34* (12), 1349−1356.

(116) Lu, Y.; Wei, J.; Shi, Y.; Jin, O.; Guo, J. Effects of fabrication condition on the network morphology and electro-optical characteristics of polymer-dispersed bistable smectic A liquid crystal device. *Liq. Cryst.* **2013**, *40*, 581.

(117) Katariya- Jain, A.; Deshmukh, R. An Overview of Polymer-Dispersed Liquid Crystal Composite Films and Their Applications. *Liq. Cryst. Display Technol.* **2020**, 11−78.

(118) Bulgakova, S. A.; Mashin, A. I.; Kazantseva, I. A.; Kashtanov, D. E.; Jones, M. M.; Tsepkov, G. S.; Korobkov, A. V.; Nezhdanov, A. V. Influence of the composition of the polymer matrix on the electrooptical properties of films with a dispersed liquid crystal. *Russian Journal of Applied Chemistry* **2008**, *81* (8), 1446−1451.

(119) Takenaka, Y.; Škarabot, M.; Muševič, I. Nematic Liquid-Crystal Necklace Structure Made by Microfluidics System. *Langmuir* **2020**, *36* (12), 3234−3241.

(120) Lagerwall, J. P. F.; McCann, J. T.; Formo, E.; Scalia, G.; Xia, Y. Coaxial electrospinning of microfibres with liquid crystal in the core. *Chem. Commun.* **2008**, No. 42, 5420−5422.

(121) Davies, M.; Hobbs, M. J.; Nohl, J.; Davies, B.; Rodenburg, C.; Willmott, J. R. Aerosol jet printing polymer dispersed liquid crystals on highly curved optical surfaces and edges. *Sci. Rep.* **2022**, *12* (1), No. 18496.

(122) Dierking, I. *Polymer-modified liquid crystals*; Royal Society of Chemistry, 2019.

(123) Ahmad, F.; Jamil, M.; Lee, J. W.; Kim, S. R.; Jeon, Y. J. The effect of UV intensities and curing time on polymer dispersed liquid crystal (PDLC) display: A detailed analysis study. *Electronic Materials Letters* **2016**, *12* (5), 685−692.

(124) Choi, S.-H.; Kim, J.-A.; Heo, G. S.; Park, H.-G. Electro-optical characteristics of polymer-dispersed liquid crystal containing copper (II) phthalocyanine as a function of UV irradiation time. *J. Mol. Liq.* **2022**, *363*, No. 119821.

(125) Nasir, N.; Kumar, S.; Kim, M.; Nguyen, V. H.; Suleman, M.; Park, H. M.; Lee, S.; Kang, D.; Seo, Y. Effect of the Photoinitiator Concentration on the Electro-optical Properties of Thiol−Acrylate-Based PDLC Smart Windows. *ACS Applied Energy Materials* **2022**, *5* (6), 6986−6995.

(126) Mucha, M. Polymer as an important component of blends and composites with liquid crystals. *Prog. Polym. Sci.* **2003**, *28* (5), 837−873.

(127) Mani, S.; Patwardhan, S.; Hadkar, S.; Mishra, K.; Sarawade, P. Effect of polymer concentration on optical and electrical properties of liquid crystals for photonic applications. *Materials Today: Proceedings* **2022**, *62*, 7035−7039.

(128) Ahmad, F.; Luqman, M.; Jamil, M. Advances in the metal nanoparticles (MNPs) doped liquid crystals and polymer dispersed liquid crystal (PDLC) composites and their applications - a review. *Mol. Cryst. Liq. Cryst.* **2021**, *731* (1), 1−33.

(129) He, Z.; Yu, P.; Zhang, H.; Zhao, Y.; Zhu, Y.; Guo, Z.; Ma, C.; Zhang, H.; Miao, Z.; Shen, W. J. N. Silicon nanostructure-doped polymer/nematic liquid crystal composites for low voltage-driven smart windows. *Nanotechnology* **2022**, *33* (8), No. 085205.

(130) Dimitrov, D. Z.; Chen, Z. F.; Marinova, V.; Petrova, D.; Ho, C. Y.; Napoleonov, B.; Blagoev, B.; Strijkova, V.; Hsu, K. Y.; Lin, S. H. ALD Deposited ZnO:Al Films on Mica for Flexible PDLC Devices. *Nanomaterials (Basel)* **2021**, *11* (4), 1011.

(131) Hsu, C. C.; Chen, Y. X.; Li, H. W.; Hsu, J. S. Low switching voltage ZnO quantum dots doped polymer-dispersed liquid crystal film. *Opt Express* **2016**, *24* (7), 7063−7068.

(132) Jayoti, D.; Malik, P.; Prasad, S. K. Effect of ZnO nanoparticles on the morphology, dielectric, electro-optic and photo luminescence properties of a confined ferroelectric liquid crystal material. *J. Mol. Liq.* **2018**, *250*, 381−387.

(133) Zhao, C.; Hu, Y.; Xu, J.; Yu, M.; Zou, C.; Wang, Q.; Gao, Y.; Yang, H. J. C. Research on the morphology, electro-optical properties and mechanical properties of electrochromic polymer-dispersed liquid crystalline films doped with anthraquinone dyes. *Crystals* **2023**, *13* (5), 735.

(134) Kumar, P.; Sharma, V.; Raina, K. J. J. o. M. L. Studies on inter-dependency of electrooptic characteristics of orange azo and blue anthraquinone dichroic dye doped polymer dispersed liquid crystals. *J. Mol. Liq.* **2018**, *251*, 407−416.

(135) Malik, M.; Bhatia, P.; Deshmukh, R. Effect of nematic liquid crystals on optical properties of solvent induced phase separated PDLC composite films. *Indian J. Sci. Technol.* **2012**, *5* (10), 1−13.

(136) Ailincai, D.; Pamfil, D.; Marin, L. Multiple bio-responsive polymer dispersed liquid crystal composites for sensing applications. *J. Mol. Liq.* **2018**, *272*, 572−582.

(137) Mert, H.; Dinçer, H.; Çalışkan, E.; Şen, B. N.; Gürsel, Y. H. Preparation of a new polymer-dispersed liquid crystal film by using phthalocyanine-functional photocurable copolymer. *J. Appl. Polym. Sci.* **2015**, *132* (10), 41574.

(138) Soulé, E. R.; Abukhdeir, N. M.; Rey, A. D. Thermodynamics, Transition Dynamics, and Texturing in Polymer-Dispersed Liquid Crystals with Mesogens Exhibiting a Direct Isotropic/Smectic-A Transition. *Macromolecules* **2009**, *42* (24), 9486−9497.

(139) Jayoti, D.; Khushboo; Malik, P.; Singh, A. Effect of polymer concentration on morphology, dielectric and optical properties in a polymer-dispersed ferroelectric liquid crystal. *Liq. Cryst.* **2016**, *43* (5), 623−631.

(140) Malik, P.; Chauhan, G.; Kumar, P.; Deep, A. Effect of polymer concentration on the electro-optical, dielectric and photolumines-cence properties of confined ferroelectric liquid crystals composites. *Liq. Cryst.* **2022**, *49* (14), 2008−2018.

(141) Jayoti, D.; Malik, P. Polymer Concentration Dependent Morphological and Electro-Optic Properties of Polymer Dispersed Ferroelectric Liquid Crystal Composites. *Macromol. Symp.* **2015**, *357* (1), 148−153.

(142) Singh, A. K.; Malik, P.; Chauhan, G.; Hegde, G.; Malik, P. Synthesis and characterization of biowaste-based porous carbon nanoparticle-polymer dispersed ferroelectric liquid crystal composites. *J. Mol. Liq.* **2023**, *390*, No. 123024.

(143) Xu, J.; Yu, M.; Zou, C.; Zhang, Z.; Gao, Y.; Zhu, S.; Yang, H. Effect of different types of mesogenic compounds with fluorine and cyano-group on the working temperature of polymer dispersed liquid crystal films. *J. Mol. Liq.* **2023**, *387*, No. 122629.

(144) Drzaic, P. S. *Liquid Crystal Dispersions*; World Scientific, 1995.

(145) De Souza Gomes, A. *New Polymers for Special Applications*; IntechOpen, 2012.

(146) Braun, D. Origins and development of initiation of free radical polymerization processes. *Int. J. Polymer Sci.* **2009**, *2009* (1), No. 893234.

(147) Colombani, D. J. P. i. p. s. Chain-growth control in free radical polymerization. *Prog. Polym. Sci.* **1997**, *22* (8), 1649−1720.

(148) Lee, M. J.; Duan, F. F.; Wu, P. C.; Lee, W. Liquid crystal-photopolymer composite films for label-free single-substrate protein quantitation and immunoassay. *Biomed Opt Express* **2020**, *11* (9), 4915−4927.

(149) Yan, J.; Fan, X.; Liu, Y.; Qu, K.; Yu, Y.; Li, R.-Z. UV-patterned polymer dispersed liquid crystals: Impact of UV curing on electro-optical properties of image-embedded smart windows. *Applied Materials Today* **2023**, *32*, No. 101840.

(150) Kim, J.; Han, J. I. Effect of liquid crystal concentration on electro-optical properties of polymer dispersed liquid crystal lens for smart electronic glasses with auto-shading and auto-focusing function. *Electronic Materials Letters* **2014**, *10* (3), 607−610.

(151) Saeed, M. H.; Zhang, S.; Zhou, L.; Chen, G.; Wang, M.; Zhang, L.; Yang, D.; Yang, H. Effects of rigid structures containing (meth)acrylate monomers and crosslinking agents with different chain length on the morphology and electro-optical properties of polymer-dispersed liquid crystal films. *Journal of Modern Optics* **2020**, *67* (8), 682−691.

(152) Lin, H.; Zhang, S.; Saeed, M. H.; Zhou, L.; Gao, H.; Huang, J.; Zhang, L.; Yang, H.; Xiao, J.; Gao, Y. Effects of the methacrylate monomers with different end groups on the morphologies, electro-optical and mechanical properties of polymer dispersed liquid crystals composite films. *Liq. Cryst.* **2021**, *48* (5), 722−734.

(153) Zhang, C.; Yu, P.; Zhao, J.; Liang, M.; He, Z.; Miao, Z. Molecular engineering controlled electric-optical performance of polymer dispersed liquid crystals. *Liq. Cryst.* **2024**, 1−11.

(154) Yu, M.; Zhou, F.; Zhang, L.; He, X.; Chen, C.; Zhang, Z.; Gao, Y.; Wang, Q.; Xiao, J.; Wei, H.; et al. Effects of hydroxylated acrylates on electro-optical performance and adhesion strength of polymer dispersed liquid crystal films. *J. Mol. Liq.* **2024**, *397*, No. 124180.

(155) Yu, M.; Xu, J.; Luo, L.; Zhang, L.; Gao, Y.; Zou, C.; Wang, Q.; Wei, H.; Wang, X.; Yang, H. Role of Hydroxy Group in the Electro-Optical Properties of Polymer-Dispersed Liquid Crystals. *Crystals* **2023**, *13*, 843.

(156) Hu, J.; Hu, W.; Zhang, S.; Sun, C.; Lan, R.; Cao, Y.; Ren, Y.; Xu, J.; Wang, X.; Saeed, M.; et al. Combined effect of hydroxylated and fluorinated acrylate monomers on improving the electro-optical and mechanical performances of PDLC-films. *Liq. Cryst.* **2022**, *49*, 769.

(157) Zhang, Y.; Zhou, L.; Yang, J.; Zhang, J.; Hai, M.; Zhang, L.; Li, F.; Zhang, C.; Yang, Z.; Yang, H.; et al. Effects of crosslinking agent/diluents/thiol on morphology of the polymer matrix and electro-optical properties of polymer-dispersed liquid crystal. *Liq. Cryst.* **2018**, *45* (5), 728−735.

(158) Stille, J. K. Step-growth polymerization. *J. Chem. Educ.* **1981**, *58* (11), 862.

(159) Macchione, M. A.; Aristizabal Bedoya, D.; Figueroa, F. N.; Strumia, M. C. Chapter 2 - Synthetic and semi-synthetic polymers for pharmaceutical applications. In *Advances and Challenges in Pharmaceutical Technology*, Nayak, A. K., Pal, K., Banerjee, I., Maji, S., Nanda, U., Eds.; Academic Press, 2021; pp 45−73.

(160) Penczek, S.; Pretula, J.; Slomkowski, S. Ring-opening polymerization. *Chem. Teacher Int.* **2021**, *3* (2), 33−57.

(161) Song, P.; Cao, H.; Wang, F.; Liu, F.; Yang, H. J. L. C. The influence of the structure of curable epoxy monomers on the electro-optical properties of polymer dispersed liquid crystal devices prepared by UV-initiated cationic polymerisation. *Liq. Cryst.* **2012**, *39* (4), 433−440.

(162) Ellahi, M.; Rafique, M.; Qadir, A.; Ali, M. F. Study on the Efects of Epoxy Resin Based PDLC Films Using Triethanolamine (TEA) as Catalyst. *Proc. AMPE* **2016**, *149*, 149−157.

(163) Saeed, M. H.; Gao, Y.; Zhou, L.; Zhong, T.; Zhang, S.; Li, C.; Zhang, L.; Yang, H. Effects of multifunctional acrylates and thiols on the morphology and electro-optical properties of polymer-dispersed liquid crystal films. *Liq. Cryst.* **2021**, *48* (10), 1457−1466.

(164) Shi, Z.; Shao, L.; Zhang, Y.; Guan, Y.; Wang, F.; Deng, F.; Liu, Y.; Wang, Y. Fabrication of polymer-dispersed liquid crystals with low

driving voltage based on the thiol-ene click reaction. *Polym. Int.* **2017**, *66* (7), 1094−1098.

(165) Ellahi, M.; Liu, F.; Song, P.; Gao, Y.; Cao, H.; Rafique, M. Y.; Khaskheli, M. A.; Zubair Iqbal, M.; Yang, H. Influence of the multi-functional epoxy monomers structure on the electro-optical properties and morphology of polymer-dispersed liquid crystal films. *Polym. Bull.* **2013**, *70*, 2967.

(166) Chen, H.; Wang, X.; Xu, J.; Hu, W.; Yu, M.; Zhang, L.; Jiang, Y.; Yang, H. A Stable PDLC Film with High Ageing Resistance from an Optimized System Containing Rigid Monomer. *Molecules* **2023**, *28* (4), 1887.

(167) He, Z.; Yu, P.; Zhao, Y.; Yang, Q.; Zhao, Y.; Zhang, H.; Zi, S.; Miao, Z.; Zhang, H.; Shen, W. The regulation of electric-optical properties of polymer-dispersed liquid crystals via implantation of polyhedral oligomeric silsesquioxane (POSS) microstructure. *Liq. Cryst.* **2022**, *49* (2), 240−247.

(168) Wu, Y.; Zhao, Y.; Gao, H.; Du, Z.; Zhang, H.; Luan, Y.; Wang, D.; Li, C. Preparation of triple-layer polymer dispersed liquid crystal films with progressive driving functionality. *Liq. Cryst.* **2023**, *50* (15), 2468−2481.

(169) Balenko, N.; Shibaev, V.; Bobrovsky, A. Mechanosensitive polymer-dispersed cholesteric liquid crystal composites based on various polymer matrices. *Polymer* **2023**, *281*, No. 126119.

(170) Kalashnikov, S. V.; Romanov, N. A.; Nomoev, A. V. Study of the properties of liquid crystals modified by nanoparticles. *J. Appl. Phys.* **2016**, *119* (9), No. 094304.

(171) Kumar, R.; Raina, K.K. Morphological control and switchable photoluminescence responses of silica nanoparticles-modified polymer-dispersed liquid crystal composite films. *Liq. Cryst.* **2015**, *42*, 119.

(172) Kumar, S.; Hong, H.; Choi, W.; Akhtar, I.; Rehman, M. A.; Seo, Y. Acrylate-assisted fractal nanostructured polymer dispersed liquid crystal droplet based vibrant colored smart-windows. *RSC Adv.* **2019**, *9* (22), 12645−12655.

(173) Ma, C.; Wu, Y.; Yu, M.; Gao, Y.; Xiao, J.; Zou, C.; Yang, H. Effect of Liquid Crystalline Acrylates on the Electro-Optical Properties and Micro-Structures of Polymer-Dispersed Liquid Crystal Films. *Crystals* **2023**, *13* (9), 1294.

(174) Yu, P.; Chen, X.; Zhang, D.; Gao, J.; Ma, C.; Zhang, C.; He, Z.; Wang, D.; Miao, Z. Polymer-Dispersed Liquid Crystal Films on Flexible Substrates with Excellent Bending Resistance and Spacing Stability. *Langmuir* **2023**, *39* (1), 610−618.

(175) Yu, M.; Xu, J.; Wang, T.; Zhang, L.; Wei, H.; Zou, C.; Gao, Y.; Yang, H. Effects of acrylate monomers with different alkyl chain structure on the electro-optical properties and microstructure of polymer dispersed liquid crystals. *J. Appl. Polym. Sci.* **2022**, *139*, No. e53056. DOI: 10.1002/app.53056.

(176) Ganesan, L. M.; Wirges, W.; Mellinger, A.; Gerhard, R. Piezo-optical and electro-optical behaviour of nematic liquid crystals dispersed in a ferroelectric copolymer matrix. *J. Phys. D: Appl. Phys.* **2010**, *43*, No. 015401.

(177) Holländer, L.; Kossack, W.; Kollosche, M.; Wirges, W.; Kremer, F.; Gerhard, R. Influence of the remanent polarisation on the liquid crystal alignment in composite films of ferroelectric poly-(vinylidene fluoride-trifluoroethylene) and a cyanobiphenyl-based liquid crystal. *Liq. Cryst.* **2016**, *43*, 1514.

(178) Shi, Z.; He, Z.; Li, C.; Miao, Z.; Wang, D.; Luan, Y.; Li, Y.; Zhao, Y. The role of nanomesh fibres loaded with BaTiO3 nanoparticles on the electro-optical performance of PDLC devices. *Applied Materials Today* **2022**, *29*, No. 101622.

(179) Liang, Z.; Zhao, Y.; Gao, H.; Wang, D.; Miao, Z.; Cao, H.; Yang, Z.; He, W. The relationship between crosslinker, liquid crystal, and magnetic nanomaterial doping on electro-optical properties of PDLC. *Liq. Cryst.* **2021**, *48* (14), 2016−2026.

(180) Kumari, A.; Sinha, A. Role of BaTiO3 nanoparticles on electro-optic performance of epoxy-resin-based PDLC devices. *Liq. Cryst.* **2021**, *48* (1), 23−34.

(181) Sharma, V.; Kumar, P. Electro-optically oriented Kerr and orientational phase study of normal mode polymer dispersed liquid

crystals — Effect of dispersion of nanoparticles. *J. Mol. Liq.* **2022**, *348*, No. 118030.

(182) Katariya Jain, A.; Deshmukh, R. Influence of a guest dichroic azo dye on a host liquid crystal dispersed in polymer matrix. *Int. J. ChemTech Res.* **2014**, *6*, 1813−1816.

(183) Shim, H.; Lyu, H.-K.; Allabergenov, B.; Garbovskiy, Y.; Glushchenko, A.; Choi, B. Switchable Response of Ferroelectric Nanoparticle Doped Polymer-Dispersed Liquid Crystals. *J. Nanosci. Nanotechnol.* **2016**, *16*, 11125−11129.

(184) Shi, Z.; He, Z.; Li, C.; Miao, Z.; Wang, D.; Luan, Y.; Li, Y.; Zhao, Y. J. A. M. T. The role of nanomesh fibres loaded with BaTiO3 nanoparticles on the electro-optical performance of PDLC devices. *Applied Materials Today* **2022**, *29*, No. 101622.

(185) Ji, Y.-Y.; Fan, F.; Zhang, X.; Cheng, J.-R.; Chang, S.-J. Terahertz birefringence anisotropy and relaxation effects in polymer-dispersed liquid crystal doped with gold nanoparticles. *Opt. Express* **2020**, *28* (12), 17253−17265.

(186) Li, S.; Fu, M.; Sun, H.; Zhao, Y.; Liu, Y.; He, D.; Wang, Y. Enhanced Photorefractive and Third-Order Nonlinear Optical Properties of 5CB-Based Polymer-Dispersed Liquid Crystals by Graphene Doping. *J. Phys. Chem. C* **2014**, *118* (31), 18015−18020.

(187) Marinova, V.; Tong, Z. F.; Petrov, S.; Karashanova, D.; Lin, Y. H.; Lin, S. H.; Hsu, K. Y. Graphene oxide doped PDLC films for all optically controlled light valve structures. *Proc. SPIE* **2016**, *9970*, 997009 DOI: 10.1117/12.2238508.

(188) Koh, W. S.; Phua, W.; Goh, W. The Potential of Graphene as a Transparent Electrode. *Optical Properties of Graphene* **2017**, 457−482.

(189) Liu, F.; Wang, G.; Pal, K.; Zhan, B.; Liu, S.; Wen, D.; Ye, S. Flexible Polymer Dispersed Liquid Crystal Module with Graphene Electrode. *J. Nanosci. Nanotechnol.* **2015**, *15* (12), 9829−9833.

(190) Tsai, T.-Y.; Lee, C.-Y.; Lee, C.-J.; Chang, W.-C.; Lee, W.; Chen, P.-C. Preparation and characterization of polymer-dispersed liquid crystal (PDLC) with different cation exchange capacity (CEC) clays. *J. Phys. Chem. Solids* **2010**, *71* (4), 595−599.

(191) John V, N.; Varanakkottu, S. N.; Varghese, S. Flexible, ferroelectric nanoparticle doped polymer dispersed liquid crystal devices for lower switching voltage and nanoenergy generation. *Opt. Mater.* **2018**, *80*, 233−240.

(192) He, T.; Yang, B.; Zhang, L.; Shi, Z.; Gong, X.; Geng, P.; Gao, Z.; Wang, Y. A study on electro-optical properties of polymer dispersed liquid crystal films doped with barium titanate nanoparticles prepared by nucleophile-initiated thiol-ene click reaction. *Liq. Cryst.* **2020**, *47* (7), 1004−1018.

(193) Shim, H.; Lyu, H.-K.; Allabergenov, B.; Garbovskiy, Y.; Glushchenko, A.; Choi, B. Switchable response of ferroelectric nanoparticle doped polymer-dispersed liquid crystals. *J. Nanosci. Nanotechnol.* **2016**, *16* (10), 11125−11129.

(194) Sharma, V.; Kumar, P.; Chinky; Gahrotra, R.; Raina, K. K.; Malik, P. Effect of nano particles on electro optic properties of polymer dispersed liquid crystal in normal mode. *AIP Conf. Proc.* **2019**, *2142*, 130002.

(195) Wang, X.; Hu, W.; Chen, H.; Saeed, M. H.; Huang, J.; Hu, J.; Ren, Y.; Xu, J.; Zhang, L.; Yu, M.; et al. Effects of chemically functionalized TiO2 nanoparticles on the UV-shielding characteristics of polymer-dispersed liquid crystals. *Polym. Adv. Technol.* **2022**, *33* (5), 1561−1568.

(196) Jinqian, L.; Zhao, Y.; Gao, H.; Wang, D.; Miao, Z.; Cao, H.; Yang, Z.; He, W. Polymer dispersed liquid crystals doped with CeO2 nanoparticles for the smart window. *Liq. Cryst.* **2022**, *49* (1), 29−38.

(197) Jayoti, D.; Malik, P.; Singh, A. Analysis of morphological behaviour and electro-optical properties of silica nanoparticles doped polymer dispersed liquid crystal composites. *J. Mol. Liq.* **2017**, *225*, 456−461.

(198) Singh, A. K.; Malik, P. Textural, electro-optical, dielectric and fluorescence studies of citrate buffer stabilized gold nanoparticles doped in polymer-dispersed liquid crystals composites. *Liq. Cryst.* **2022**, *49* (6), 864−874.

(199) Kumar, P.; Sharma, V.; Raina, K. Studies on inter-dependency of electrooptic characteristics of orange azo and blue anthraquinone dichroic dye doped polymer dispersed liquid crystals. *J. Mol. Liq.* **2018**, *251*, 407.

(200) Katariya-Jain, A.; Mhatre, M. M.; Dierking, I.; Deshmukh, R. R. Enhanced thermo-electro-optical and dielectric properties of carbon nanoparticle-doped polymer dispersed liquid crystal based switchable windows. *J. Mol. Liq.* **2024**, *393*, No. 123575.

(201) Sharma, V.; Kumar, P.; Sharma, A.; Chinky; Raina, K. K. Droplet configuration control with orange azo dichroic dye in polymer dispersed liquid crystal for advanced electro-optic characteristics. *J. Mol. Liq.* **2017**, *233*, 122−130.

(202) Önsal, G.; Kocakülah, G.; Kahyaoğlu, A.; Köysal, O. Influence of azo dye concentration on dielectric response in polymer dispersed liquid crystal composites. *J. Mol. Liq.* **2019**, *284*, 607−615.

(203) Jiang, Z.; Zheng, J.; Liu, Y.; Zhu, Q. Investigation of dielectric properties in polymer dispersed liquid crystal films doped with CuO nanorods. *J. Mol. Liq.* **2019**, *295*, No. 111667.

(204) Shivaraja, S. J.; Gupta, R. K.; Manjuladevi, V. Faster switching polymer dispersed liquid crystal devices incorporated with functionalized SWCNTs. *J. Mol. Liq.* **2022**, *354*, No. 118905.

(205) Gandhi, S. S.; Chien, L.-C. High transmittance optical films based on quantum dot doped nanoscale polymer dispersed liquid crystals. *Opt. Mater.* **2016**, *54*, 300−305.

(206) Wang, L.; Meng, F.; Sun, Y.; Yang, H. Effect of surfactant-modified ZnS:Mn nanoparticles on the electro-optical properties of composite polymer-dispersed liquid crystal films. *Composites Part B: Engineering* **2013**, *45* (1), 780−784.

(207) Shaik, S.; Nundy, S.; Maduru, V. R.; Ghosh, A.; Afzal, A. Polymer dispersed liquid crystal retrofitted smart switchable glazing: Energy saving, diurnal illumination, and CO2 mitigation prospective. *Journal of Cleaner Production* **2022**, *350*, No. 131444.

(208) Guo, S.-M.; Liang, X.; Zhang, C.-H.; Chen, M.; Shen, C.; Zhang, L.-Y.; Yuan, X.; He, B.-F.; Yang, H. Preparation of a Thermally Light-Transmittance-Controllable Film from a Coexistent System of Polymer-Dispersed and Polymer-Stabilized Liquid Crystals. *ACS Appl. Mater. Interfaces* **2017**, *9* (3), 2942−2947.

(209) Wu, K.; Sun, J.; Meng, F.; Fan, M.; Kong, X.; Cai, M.; Zhao, T.; Yang, C.; Xin, Y.; Xing, J.; et al. Highly flexible and electrically controlled grating enabled by polymer dispersed liquid crystal. *J. Mol. Liq.* **2022**, *353*, No. 118664.

(210) Tseng, H.-Y.; Chang, L.-M.; Lin, K.-W.; Li, C.-C.; Lin, W.-H.; Wang, C.-T.; Lin, C.-W.; Liu, S.-H.; Lin, T.-H. Smart Window with Active-Passive Hybrid Control. *Materials* **2020**, *13* (18), 4137.

(211) Huang, J.; Li, J.; Xu, J.; Wang, Z.; Sheng, W.; Li, H.; Yang, Y.; Song, W. Simultaneous achievement of high visible transmission and near-infrared heat shielding in flexible liquid crystal-based smart windows via electrode design. *Sol. Energy* **2019**, *188*, 857−864.

(212) Kim, Y.; Kim, K.; Kim, K. B.; Park, J.-Y.; Lee, N.; Seo, Y. Flexible polymer dispersed liquid crystal film with graphene transparent electrodes. *Curr. Appl. Phys.* **2016**, *16* (3), 409−414.

(213) Muhsin, B.; Roesch, R.; Gobsch, G.; Hoppe, H. Flexible ITO-free polymer solar cells based on highly conductive PEDOT:PSS and a printed silver grid. *Sol. Energy Mater. Sol. Cells* **2014**, *130*, 551−554.

(214) Khaligh, H. H.; Liew, K.; Han, Y.; Abukhdeir, N. M.; Goldthorpe, I. A. Silver nanowire transparent electrodes for liquid crystal-based smart windows. *Sol. Energy Mater. Sol. Cells* **2015**, *132*, 337−341.

(215) Liang, X.; Lu, J.; Zhao, T.; Yu, X.; Jiang, Q.; Hu, Y.; Zhu, P.; Sun, R.; Wong, C.-P. Facile and Efficient Welding of Silver Nanowires Based on UVA-Induced Nanoscale Photothermal Process for Roll-to-Roll Manufacturing of High-Performance Transparent Conducting Films. *Advanced Materials Interfaces* **2019**, *6*, No. 1801635.

(216) Biswas, S. K.; Sano, H.; Yang, X.; Tanpichai, S.; Shams, M. I.; Yano, H. Highly Thermal-Resilient AgNW Transparent Electrode and Optical Device on Thermomechanically Superstable Cellulose Nanorod-Reinforced Nanocomposites. *Advanced Optical Materials* **2019**, *7* (15), No. 1900532.

(217) Dimitrov, D. Z.; Chen, Z. F.; Marinova, V.; Petrova, D.; Ho, C. Y.; Napoleonov, B.; Blagoev, B.; Strijkova, V.; Hsu, K. Y.; Lin, S. H.; et al. ALD Deposited ZnO:Al Films on Mica for Flexible PDLC Devices. *Nanomaterials* 2021, 11 (4), 1011.

(218) Jung, D.; Choi, W.; Park, J.-Y.; Kim, K.; Lee, N.; Seo, Y.; Kim, H.; Kong, N. K. Experimental Data of Inorganic Gel based Smart Window using Silica Sol-Gel process. *Data in Brief* 2016, 9, 716.

(219) Kim, E. M.; Kim, S. J.; Choi, G. B.; Lee, J.; Koo, M. M.; Kim, J.; Kim, Y. W.; Lee, J.; Kim, J. H.; Seo, T. H. A Graphene-Based Polymer-Dispersed Liquid Crystal Device Enabled through a Water-Induced Interface Cleaning Process. *Nanomaterials* 2023, 13 (16), 2309.

(220) Zhang, H.; Zhu, X.; Tai, Y.; Zhou, J.; Li, H.; Li, Z.; Wang, R.; Zhang, J.; Zhang, Y.; Ge, W.; et al. Recent advances in nanofiber-based flexible transparent electrodes. *International Journal of Extreme Manufacturing* 2023, 5 (3), No. 032005.

(221) Mondal, I.; S, K.; Ganesha, M. K.; Baral, M.; Kumar, A.; Vimala, S.; Madhuri, P. L.; Nair, G. G.; Prasad, S. K.; Singh, A. K.; et al. ITO-free large area PDLC smart windows: a cost-effective fabrication using spray coated SnO2 on an invisible Al mesh. *J. Mater. Chem. A* 2021, 9 (40), 23157−23168.

(222) Park, J.-Y.; Kim, H.-K. Highly stretchable polymer-dispersed liquid crystal-based smart windows with transparent and stretchable hybrid electrodes. *RSC Adv.* 2018, 8 (64), 36549−36557.

(223) Nasir, N.; Hong, H.; Rehman, M. A.; Kumar, S.; Seo, Y. Polymer-dispersed liquid-crystal-based switchable glazing fabricated via vacuum glass coupling. *RSC Adv.* 2020, 10 (53), 32225−32231.

(224) Kumar, S.; Kang, D.; Nguyen, V. H.; Nasir, N.; Hong, H.; Kim, M.; Nguyen, D. C.; Lee, Y.-j.; Lee, N.; Seo, Y. Application of Titanium-Carbide MXene-Based Transparent Conducting Electrodes in Flexible Smart Windows. *ACS Appl. Mater. Interfaces* 2021, 13 (34), 40976−40985.

(225) Ghosh, A. Investigation of vacuum-integrated switchable polymer dispersed liquid crystal glazing for smart window application for less energy-hungry building. *Energy* 2023, 265, No. 126396.

(226) Mesloub, A.; Ghosh, A.; Kolsi, L.; Alshenaifi, M. Polymer-Dispersed Liquid Crystal (PDLC) smart switchable windows for less-energy hungry buildings and visual comfort in hot desert climate. *Journal of Building Engineering* 2022, 59, No. 105101.

(227) Hemaida, A.; Ghosh, A.; Sundaram, S.; Mallick, T. K. Evaluation of thermal performance for a smart switchable adaptive polymer dispersed liquid crystal (PDLC) glazing. *Sol. Energy* 2020, 195, 185−193.

(228) Qahtan, A. M.; Almawgani, A. H. M.; Ghosh, A. Smart double glazing integrated polymer dispersed liquid crystal for enhancing building's thermal performance in hot-arid climate. *Journal of Building Engineering* 2023, 80, No. 107971.

(229) Hemaida, A.; Ghosh, A.; Sundaram, S.; Mallick, T. K. Simulation study for a switchable adaptive polymer dispersed liquid crystal smart window for two climate zones (Riyadh and London). *Energy and Buildings* 2021, 251, No. 111381.

(230) Shaik, S.; Gorantla, K.; M, V. R.; Mishra, S.; Kulkarni, K. S. Thermal and cost assessment of various polymer-dispersed liquid crystal film smart windows for energy efficient buildings. *Constr. Build. Mater.* 2020, 263, No. 120155.

(231) Xu, J.; Zhang, Z.; He, L.; Shi, Y.; Gao, Y.; Yu, M.; Yang, H. Liquid crystal/polymer composites for energy-efficient smart windows with a wide working temperature range and low off-axis haze. *Composites Part A: Applied Science and Manufacturing* 2024, 178, No. 107976.

(232) Kaur, M.; Malik, P. New graphene oxide doped polymer dispersed liquid crystal nanocomposites targeted to eco-friendly and energy-efficient smart windows. *J. Mol. Liq.* 2024, 410, No. 125565.

(233) Deng, Y.; Yang, Y.; Xiao, Y.; Xie, H.-L.; Lan, R.; Zhang, L.; Yang, H. Ultrafast Switchable Passive Radiative Cooling Smart Windows with Synergistic Optical Modulation. *Adv. Funct. Mater.* 2023, 33 (35), No. 2301319.

(234) Ube, T.; Imai, J.; Yoshida, M.; Fujisawa, T.; Hasebe, H.; Takatsu, H.; Ikeda, T. Sunlight-driven smart windows with polymer/

liquid crystal composites for autonomous control of optical properties. *Journal of Materials Chemistry C* 2022, 10 (35), 12789−12794.

(235) Wang, B.; Ye, M.; Honma, M.; Nose, T.; Sato, S. Liquid Crystal Lens with Spherical Electrode. *Jpn. J. Appl. Phys.* 2002, 41 (11A), L1232.

(236) Ren, H.; Wu, S.-T. Tunable electronic lens using a gradient polymer network liquid crystal. *Appl. Phys. Lett.* 2003, 82 (1), 22−24.

(237) Ye, M.; Sato, S. Optical Properties of Liquid Crystal Lens of Any Size. *Jpn. J. Appl. Phys.* 2002, 41 (5B), L571.

(238) Kao, Y.-Y.; Chao, P. C. P.; Hsueh, C.-W. A new low-voltage-driven GRIN liquid crystal lens with multiple ring electrodes in unequal widths. *Opt. Express* 2010, 18 (18), 18506−18518.

(239) Hsu, C. J.; Selvaraj, P.; Huang, C. Y. Low-voltage tunable liquid crystal lens fabricated with self-assembled polymer gravel arrays. *Opt. Express* 2020, 28 (5), 6582−6593.

(240) Pagidi, S.; Manda, R.; Bhattacharyya, S. S.; Lee, S. G.; Song, S. M.; Lim, Y. J.; Lee, J. H.; Lee, S. H. Fast Switchable Micro-Lenticular Lens Arrays Using Highly Transparent Nano-Polymer Dispersed Liquid Crystals. *Advanced Materials Interfaces* 2019, 6 (18), No. 1900841.

(241) Yan, J.; Fan, X.; Liu, Y.; Yu, Y.; Fang, Y.; Li, R.-Z. J. C. O. L. Passive patterned polymer dispersed liquid crystal transparent display. *Chinese Optics Letters* 2022, 20 (1), No. 013301.

(242) Su, C. W.; Liao, C. C.; Chen, M. Y. Color Transparent Display Using Polymer-Dispersed Liquid Crystal. *Journal of Display Technology* 2016, 12 (1), 31−34.

(243) Cong, S.; Cao, Y.; Fang, X.; Wang, Y.; Liu, Q.; Gui, H.; Shen, C.; Cao, X.; Kim, E. S.; Zhou, C. Carbon Nanotube Macroelectronics for Active Matrix Polymer-Dispersed Liquid Crystal Displays. *ACS Nano* 2016, 10 (11), 10068−10074.

(244) Jiang, J.; McGraw, G.; Ma, R.; Brown, J.; Yang, D.-K. Selective scattering polymer dispersed liquid crystal film for light enhancement of organic light emitting diode. *Opt. Express* 2017, 25 (4), 3327−3335.

(245) Zhou, L.; He, Z.; Han, C.; Zhang, L.; Yang, H. Switchable anti-peeping film for liquid crystal displays from polymer dispersed liquid crystals. *Liq. Cryst.* 2019, 46 (5), 718−724.

(246) Xian, H.; Li, L.; Ding, Y.; Chu, M.; Ye, C. Preparation and Orthogonal Analysis for Dual-Responsive Electrochromic Polymer Dispersed Liquid Crystal Devices. *Polymers* 2023, 15 (8), 1860.

(247) Cheng, Z.; Wang, T.; Li, X.; Zhang, Y.; Yu, H. NIR−Vis−UV Light-Responsive Actuator Films of Polymer-Dispersed Liquid Crystal/Graphene Oxide Nanocomposites. *ACS Appl. Mater. Interfaces* 2015, 7 (49), 27494−27501.

(248) Pan, J.; Liu, S.; Yang, Y.; Lu, J. A Highly Sensitive Resistive Pressure Sensor Based on a Carbon Nanotube-Liquid Crystal-PDMS Composite. *Nanomaterials* 2018, 8 (6), 413.

(249) Pagidi, S.; Pasupuleti, K. S.; Reddeppa, M.; Ahn, S.; Kim, Y.; Kim, J.-H.; Kim, M.-D.; Lee, S. H.; Jeon, M. Y. Resistive type NO2 gas sensing in polymer-dispersed liquid crystals with functionalized-carbon nanotubes dopant at room temperature. *Sens. Actuators, B* 2022, 370, No. 132482.

(250) Lai, Y.-T.; Kuo, J.-C.; Yang, Y.-J. Polymer-dispersed liquid crystal doped with carbon nanotubes for dimethyl methylphosphonate vapor-sensing application. *Appl. Phys. Lett.* 2013, 102 (19), 191912 DOI: 10.1063/1.4804297.

(251) Lai, Y.-T.; Kuo, J.-C.; Yang, Y.-J. A novel gas sensor using polymer-dispersed liquid crystal doped with carbon nanotubes. *Sensors and Actuators A: Physical* 2014, 215, 83−88.

(252) Liu, Y.; Zheng, J.; Jiang, Z.; Zhu, Q.; Chen, Q.; Zhuang, S. J. L. C. Optical and dielectric analysis of ZnO nanorods doped polymer dispersed liquid crystal and ethanol gas sensing investigation. *Liq. Cryst.* 2020, 47 (14−15), 2247−2256.

(253) Song, M.; Seo, J.; Kim, H.; Kim, Y. Ultrasensitive Multi-Functional Flexible Sensors Based on Organic Field-Effect Transistors with Polymer-Dispersed Liquid Crystal Sensing Layers. *Sci. Rep.* 2017, 7 (1), 2630.

(254) Wang, Z.; Cao, M.; Shao, G.; Zhang, Z.; Yu, H.; Chen, Y.; Zhang, Y.; Li, Y.; Xu, B.; Wang, Y.; et al. Coherent Random Lasing in Colloidal Quantum Dot-Doped Polymer-Dispersed Liquid Crystal with Low Threshold and High Stability. *J. Phys. Chem. Lett.* **2020**, *11* (3), 767−774.

(255) Yang, D.-C. J.; Cai, J.-M.; Yang, Y.-J. J. A tunable magnetic axis microdevice using polymer-dispersed liquid crystal doped with magnetic nanoparticles. *Appl. Phys. Lett.* **2018**, *113* (16), 161901 DOI: 10.1063/1.5050266.